Diploma Thesis

Stem cells in wound healing

submitted by

Alexander Helmer

for the acquisition of the academic degree

Doktor der gesamten Heilkunde
(Dr. med. univ.)

at the
Medical University of Graz

performed at the
Division of Plastic, Aesthetic & Reconstructive Surgery Graz
and the
Division of Cell Biology, Histology & Embryology

under the supervision of

Dr. Med. Univ. Alexandru-Christian Tuca
&
Ao.Univ.-Prof. Mag. Dr.rer.nat. Ingrid Lang-Olip

Graz, am 24.03.2021

STATUTORY DECLARATION

I declare that I have authored this thesis independently, that I have not used other than the declared sources / resources, and that I have explicitly marked all material which has been quoted either literally or by content from the used sources.

Graz, am 24.03.2021 Alexander Helmer eh

Acknowledgment:

Reminiscing about the time I spend on this project I realize how many people I am thankful for their help but cannot name all of them.

First, I would like to thank Ingrid Lang-Olip for helping me with my first steps into scientific work, with overcoming every problem I faced and for her mentoring skills which helped me manage the workload.

Further, I would like to thank Alexandru Tuca for supervising my progress, helping me whenever he could and his endurance with my amount of questions.

Special thanks to Eva Vonbrunn, Monika Sundl and Melanie Pichlsberger for the great cooperation during the test phase.

Content:

Abbreviations:

%GRAN *percentage of granulocytes*
%LYN *percentage of lymphocytes*
%MON *percentage of monocytes*
ADP *adenosine diphosphate*
AEC *amniotic epithelials cells*
AM *amnion membrane*
AMSC *Amnion derived mesenchymal stroma cells*
bFGF *basis fibroblast growth factor*
CD *cluster of differentiation*
Dermabond® *2-octylcynoacrylate*
ECM *extracellular matrix*
EDTA *Ethylenediaminetetraacetic acid*
GRAN *granulocytes*
HGB *haemoglobin*
IL *interleukin*
KGF *keratinocyte-derived growth factor*
M1 *pro-inflammatory macrophages*
M2 *reparative phenotype of macrophages*
MCH *mean corpuscular haemoglobin*
MCV *mean corpuscular volume*
MON *monocytes*
MPV *mean platelet volume*
MSC *mesenchymal stromal cells*
NOS2A *Nitric oxide synthase 2*
PCL *Polycaprolactone*
PCT *platelet haematocrit*
PDGF *platelet derived growth factor*
PDW *platelet distribution width*
PLA *Polylactide*
PLT *platelets*
RBC *erythrocytes*
RDW *erythrocyte distribution width*
SC *stem cells*
TGF-β *transforming growth factor beta*
VEGF *vascular endothelial growth factor*
WBC *white blood cells*

List of Illustrations:

List of tables:

Zusammenfassung:

Amnion-abgeleitete mesenchymale Stromazellen (=AMSC) sind eine intensiv untersuchte und bisher nur teilweise verstandene, vielseitig eingesetzte Hoffnung in der Medizin. Ihre entzündungshemmenden, neo-vaskulären, zellstimulierenden und Wundheilung fördernden Eigenschaften sind in vielen verschiedenen Studien nachgewiesen worden. Das Ziel dieser Studie war es in einem in vivo Mausmodell das Wundmaterial für AMSC zu finden, welches das Heilungspotential bestmöglich unterstützt. Insgesamt arbeiteten wir mit 16 Mäusen in zwei Studienzyklen, in denen jeder Maus zwei 8 mm Stanzbiopsie-Wunden auf dem Rücken verabreicht wurden. In der Pilotstudie verglichen wir verschiedene Kombinationen von Matriderm®, Matrigel® und PCL/PLA mit oder ohne AMSC. Im zweiten Zyklus definierten wir eine unbehandelte Kontrollgruppe. In beiden Durchläufen sammelten wir Blutproben, machten Fotos für die makroskopische Vermessung und entfernten die Wunden für die histologische Aufarbeitung. Zusätzlich nutzten wir Ultraschall an einer Maus für zusätzliche Einblicke in den Wundheilungsprozess. In der Pilotstudie wurden alle Mäuse am 14. Tag geopfert. Während hingegen im zweiten Zyklus wurden jeweils 3 Mäuse am 3., 7. und 14. Tag geopfert, um ein besseres Verständnis der Entzündung histologisch und aus den Blutparametern zu bekommen. Die mit Matriderm®+ Matrigel®, Matriderm®+ Matrigel®+ AMSC und PCL/PLA+ Matrigel®+ AMSC behandelten Wunden zeigten makroskopisch eine beschleunigte Wundheilung und unter mikroskopischer Beurteilung eine weiter fortgeschrittene Reepithelialisierung. Darüber hinaus zeigten die Ergebnisse der Blutproben, dass die Entzündungswerte, der mit AMSC behandelten Wunden niedriger waren, verglichen zur Kontrollgruppe und ab dem 7. Tag die Entzündung am Abklingen war. Zusammenfassend lässt sich sagen, dass Matriderm® und PCL/PLA vielversprechende Träger für AMSC zu sein scheinen. Darüber hinaus scheint Matrigel® eine positive Wirkung auf die Wundheilung und AMSC zu haben. Es müssen weitere Studien durchgeführt werden, um das vielversprechendste

Anwendungsmaterial mit statistischer Signifikanz zu untermauern und zu klinischen Studien zu gelangen.

Abstract:

Amnion derived mesenchymal stroma cells (=AMSC) are an intensely studied and, yet just partially understood, ubiquitous applicable hope in medicine. Their anti-inflammatory, neo-vascular and cell stimulating properties, promoting wound healing, have been proven in many different studies.
The objective of this study was to find the best possible application material for AMSC promoting their curing potential in an in vivo mouse model. In total we worked with 16 mice in two study cycles in which each mouse got two 8mm punch biopsy-wounds administered on their back. In the pilot study we compared different combinations of Matriderm®, Matrigel® and PCL/PLA with or without AMSC. In the second cycle we established a control group which we left untreated. In both rounds we gathered blood-samples, took photos for macroscopic assessment, and excised the wounds for microscopic evaluation. Additionally, we used ultrasonography on one mouse for additional insight concerning the wound-healing process. In the Pilot study all mice were sacrificed on the 14th day. Whereas, in the first experimental run 3 mice were sacrificed on the 3rd, on the 7th and on the 14th day to gain data on the inflammation histologically and from the blood parameters. Wounds treated with Matriderm®+ Matrigel®, Matriderm®+ Matrigel® + AMSC and PCL/PLA+ Matrigel®+ AMSC showed an accelerated wound healing macroscopically and a further progressed re-epithelialization under microscopic evaluation. Additionally, the infection parameters from the blood-samples taken from the wounds treated with AMSC are lower compared to the control group and the infection seems to end on the 7th day. Concluding, Matriderm® and PCL/PLA seem to be promising carrier for AMSC. Additionally, Matrigel® seems to have a beneficial effect on wound healing and AMSC. Further studies need to be done to determine the most promising application material with statistical significance and to advance to clinical trials.

1. Introduction

The skin, as the biggest organ of the human body, has an incomparable function as the first layer of our immune system, as thermal balance, to regulate our fluid balance, and as protection against mechanical forces. Through wounds all those functions can be endangered[1]. Wounds can be subdivided into traumatic, iatrogenic, and chronic wounds among which traumatic wounds have the highest occurrence. Iatrogenic summarizes all wounds which appear during surgical, diagnostic, or therapeutic procedures. Wounds which have no healing tendency after 4 weeks are defined as chronic wounds[2]. Unfortunately, deviations in the strictly controlled phases of wound healing can occur in any phase. Hence, understanding, influence or control chronic wounds is only partly possible. Therefore, those kinds of wounds cause significant additional costs and workload for the medical system and the individual caregivers and doctors. Wound management and wound care are estimated to cost the overall medical system 3% of its budget. In Europe alone live around 1.5 to 2 million people with chronic wounds. For example, the costs for the treatment of diabetic foot ulcers solely are about 4 to 6 billion/year[3].[4] Austrians have a life expectancy at age 65 of further 17.7 to 21.2 years but only around 8 without chronic diseases[5]. Consequently, being able to prolong the years in health would benefit not only the patient but also the medical system.

Wound healing

Depending on the literature wound healing is divided in 3 or 4 phases: Inflammation, Proliferation, Epithelialization, and Remodelling/Maturation. The different steps are based on a finely coordinated process, which depends on many different cell types, mediators, cytokines, and growth hormones. Still, they can

occur independently, and simultaneously in different areas of the wound, depending on its size and origin (Fig. 1).

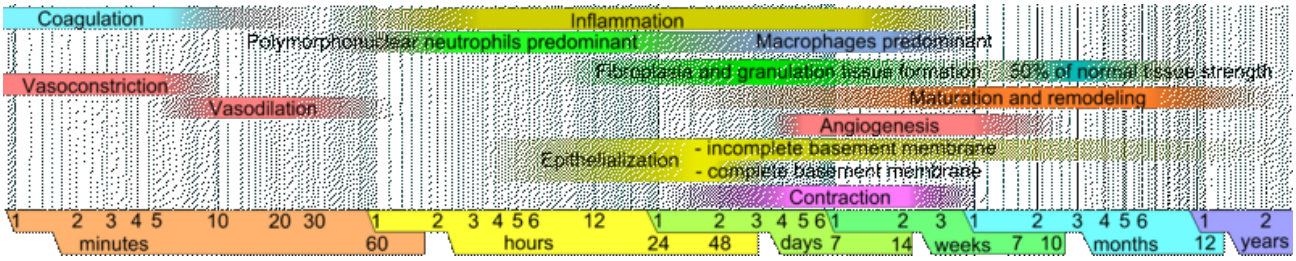

Figure 1phases of wound healing in skin over the period of 2 years [37]

Inflammation

First, vasoconstriction confines blood loss. After 5 to 10 minutes the initial blockade loosens up and blood platelets aggregate to form a clot, in response to exposed collagen and adenosine diphosphate (=ADP) of epidermal skin cells. Meanwhile, platelet-derived growth factor (=PDGF) and transforming growth factor beta (=TGF-β) is released. Consequently, neutrophil granulocytes follow the increasing gradient of chemokines. Those cells have a wide influence on the wound site. Primarily, they phagocyte dead tissue and bacterial particles. Additionally, to ensure a bacteriostatic environment they release reactive oxygen species, interleukin (IL)-1, which is proinflammatory and a stimulus for proliferation of keratinocytes. The inflammation is further supported by regulatory T cells, which reduce the interferon-gamma production, and pro-inflammatory macrophages. Within 24 to 72 hours more and more macrophages migrate into the wound, establishing homeostasis, and downregulating the inflammatory response[1, 6].

Proliferative phase

Macrophages are the key cell in this phase due to versatile abandonments (Fig. 2). The switch between the pro-inflammatory macrophages (=M1) to the reparative phenotype of macrophages (=M2) is associated with the transition between the inflammatory and proliferative phase. M2 secrete PDGF which triggers proteoglycan and collagen formation for the extracellular matrix (=ECM), and collagen production in fibroblasts and their transformation in myofibroblasts. In addition, the macrophages phagocyte the neutrophil granulocytes, bacteria, and cell debris to further hinder inflammation. Through keratinocyte-derived growth factor (=KGF), produced by fibroblasts, epithelialization from keratinocytes is stimulated. Angiogenesis is promoted through vascular endothelial growth factor (=VEGF) and basis fibroblast growth factor (bFGF) excreted by endothelial cells[1, 6].

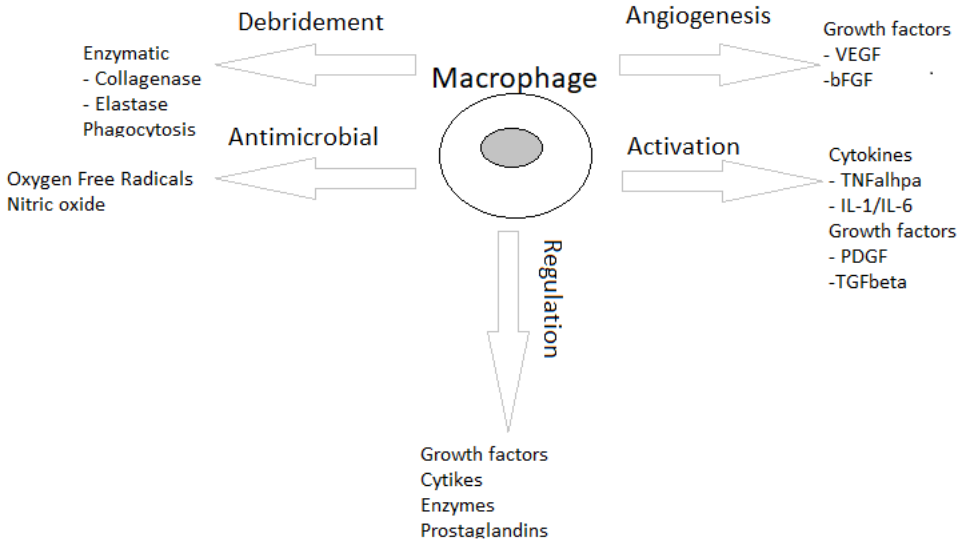

Figure 2 Systematic illustration of the macrophages' role during wound healing

Epithelialization

The process of re-epithelialization is described by different theories focusing on the migration of cells from the wound margin to the centre. The initial descriptions were leapfrogging cells, characterised through cells gradually falling over each other, and leader cells carrying a series of cells over the deepithelialized area. Additionally, three new theories might be involved, too. Activated keratinocytes form an epidermal tongue, over which more cells follow in the wound area, dragging more cells out of the blood clot-derived fibrin, fibronectin, and vitronectin (=lamellipodial crawling), and through shape changing, looser cell-cell contact and rearrangement the cells at the front shuffle with the new migrated cells (=shuffling). Finally, through contact between the migrating cells the process is stopped. The reduced number of cells, due to the injury, is substituted through invading adult stem cells from the hair follicle bulge and the interfollicular epidermis niche. Re-epithelialization is responsible for 80% of wound closure and 20% through skin contraction. For effective and complete epithelialization an appropriate ECM is the basic condition. This facilitates the possibility for keratinocyte migration. Dermis, fascia, or muscle are an ideal base for epithelialization, whereas adipose tissue is counterproductive. For most connective tissues granulation tissue needs to be formed as an underlying substrate[1, 6].

Remodelling/Maturation

The remodelling of the scar last approximately from the 3rd week till 1 year after wounding and is characterised by a change in scar size, and colour. A scar lacks epidermal appendages and is composed of densely packed collagen structure, which differs from uninjured skin. Fibroblasts play a key role in this phase. On

the first day, fibroblasts at the wound margin are stimulated by mechanical tension and PDGF, and transform into stress-fibre expressing protomyofibroblasts, which can be found in early granulation tissue. In consequence of mechanical tension, activated TGF-beta, and the splice variant EDA fibronectin trigger protomyofibroblasts evolve in α-smooth muscle actin-expressing myofibroblasts. Due to focal adhesion contacts which connects the intracellular cytoskeleton to the ECM, wound contraction appears. During this evolution of the cells a change in the collagen network of the surrounding tissue appears, too. Type 3 collagen changes to type 1 collagen, which is relatively thicker[7]. After secretion of type 3 collagen the mechanical resilience grows because of crosslinking and alignment of the initial parallel structured network. The amount of collagen increases continuously for the first three weeks, whereas the strength of the tissue reaches 70% after 6 weeks, and 80% to 90% at full maturation compared to unwounded skin. Additionally, the red colour of the early scar, due to its dense capillary network, fades away as the capillaries regress during the maturation. Consequently, the scar presents its true colour after approximately one year[1, 6].

Stem cells

Per definition stem cells (=SC) have the key capability of self-renewal and the in vivo and in vitro restoration of a specialized tissue through differentiation. First, SC are subdivided in embryonic stem cells and adult SC. Additionally, it is possible to distinguish toti-, pluri-, multi-, and unipotent SC. These potentials describe the range of abilities in which the cells can differentiate (Fig. 3). Totipotent is the first level during the growth and differentiation of the fertilized oocyte (=zygote) and the eight-cell embryo. Pluripotent SC function as the base for all cells, somatic and germline, and are found in the blastocyst's inner cell mass and in postnatal adult tissue. In adult tissue, mostly with a rapid cell

turnover, multi- or unipotent adult SC can be found. Multipotent stem cells can differentiate in a certain line, for example a haematopoietic multipotent stem cell. Unipotent stem cells only produce one sort of cell. Even though, they still have the capability to self-renewal and restoration their range of differentiation is reduced. They can be found in niches with specific microenvironment which regulates and controls their activity in most organs and tissues. The pedigree of cells got an addition in 2006 when somatic cells returned to a state of pluripotency through in vitro genetic manipulation and, consequently, underwent differentiation into cells of all germ layers[8]. In the 1970s the first mesenchymal stromal cells (=MSC) were isolated from bone marrow. Their characteristic criteria were a spindle-like shape, their ability of one single cell to build colonies, and their capability to further develop into adipocytes, chondrocytes, osteocytes, and fibrous tissue, in vitro and in vivo. Additionally, further nonhematopoietic multipotent stromal cells were found in adult adipose tissue and dermal skin tissue, as well as, in embryonic and fetal sources as amniotic membrane, umbilical cord, and umbilical cord blood/ Wharton's jelly[9]. In order to standardize the definition of MSC the International Society of Cellular Therapy stated 3 key character traits:

MSC must be plastic-adherent when maintained in standard culture conditions.

MSC must express cluster of differentiation (=CD)105, CD73 and CD90, and lack expression of CD45, CD34, CD14 or CD11b, CD79α or CD19 and HLA-DR (=Human Leukocyte Antigen – DR isotype) surface molecules.

MSC must differentiate to osteoblasts, adipocytes and chondroblasts in vitro[10].

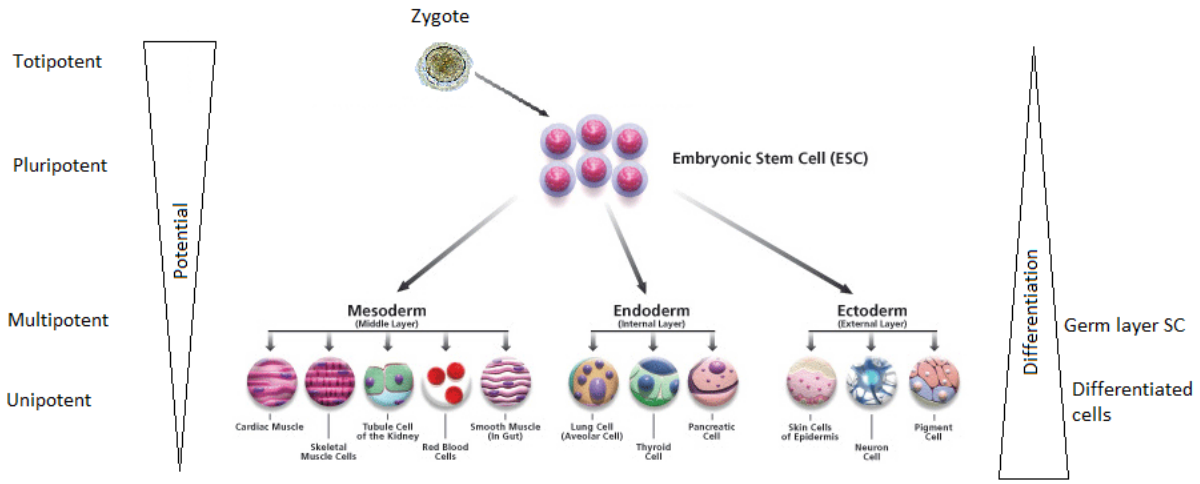

Figure 3 Schematic figure of stem cell differentiation from totipotent till specialized adult cells [38]

Influence of MSC on wound healing

MSC contribute to wound healing through different cellular mechanisms. Studies have shown that through MSC there is a higher secretion of anti-inflammatory molecule IL-10 and a decrease in inflammatory-stimulant, IL-1, IL-1β, IL-6, TNF-α, and Nitric oxide synthase 2 (=NOS2A). Additionally, MSC help shielding the wound-site through an upregulation of antimicrobial activity. Not only promote MSC the secretion of antimicrobial factors like IL-37, but they also might play a role in the M1/M2 polarization of macrophages during wound healing. Through paracrine secretion, differentiation, and secretion themselves MSC support neovascularization through a higher level of VEGF and angiopoeitin-1. Furthermore, another study suggested that MSC might act as pericytes to stabilize the blood vessel formation[11]. Supplementary, MSC stimulate adult epidermal stem cells to differentiate[12].

Human amnion derived mesenchymal stem cells

MSC from the amnion are gathered from the amnion membrane (=AM). The AM forms the most inner layer of the amnion cavity and covers the chorionic plate of the placenta. It can be dissected directly postpartum (Fig. 4). Consequently, it has direct contact with the foetus and the amniotic fluid. The AM itself is structured in 5 layers: epithelium layer, basement membrane, compact layer, fibroblast layer, and spongy layer. Additionally, amniotic mesenchymal stromal cells (=AMSC) and amniotic epithelial cells (=AEC) are contained in the AM. AEC express surface markers associated with embryonic stem cells (SSEA-3, SSEA-4, TRA-1-60, TRA-1-81) and pluripotent stem cells-specific transcription factors (Oct-4 and Nanog). Additionally, for immune tolerance and anti-inflammatory properties, human leukocyte antigen G (HLA-G), secretory leukocyte proteinase inhibitor (=SLPI), elafin, and β-defensins. AMC can be the base for all three germ layers and can play an essential role in wound healing through secretion of anti-inflammatory cytokines (PGE2, IDO, HGF and TGF-β) and angiogenic factors (VEGF, PDGF)[13]. The usage of amniotic membrane in therapy was first described by Davis 1910 as skin transplant[14]. In 1940 De Rotth used it to treat symblepharon or entropion after chemical burns[15]. Additionally, amnion was used in a variety of studies as a therapy of non-healing skin ulcers, vaginal reconstruction, repair of abdominal herniation, closure of pericardium and prevention of surgical adhesion. In the search for stem cells researchers became more interested in foetal sources like Wharton's jelly, placenta or amniotic membrane[16]. After finding sources the regenerative medicine focused on combining knowledge of tissue engineering, material sciences, genetics & molecular biology, cell, tissue & organ transplantation, and developmental biology to find the perfect usage of the newly found therapeutic possibility.

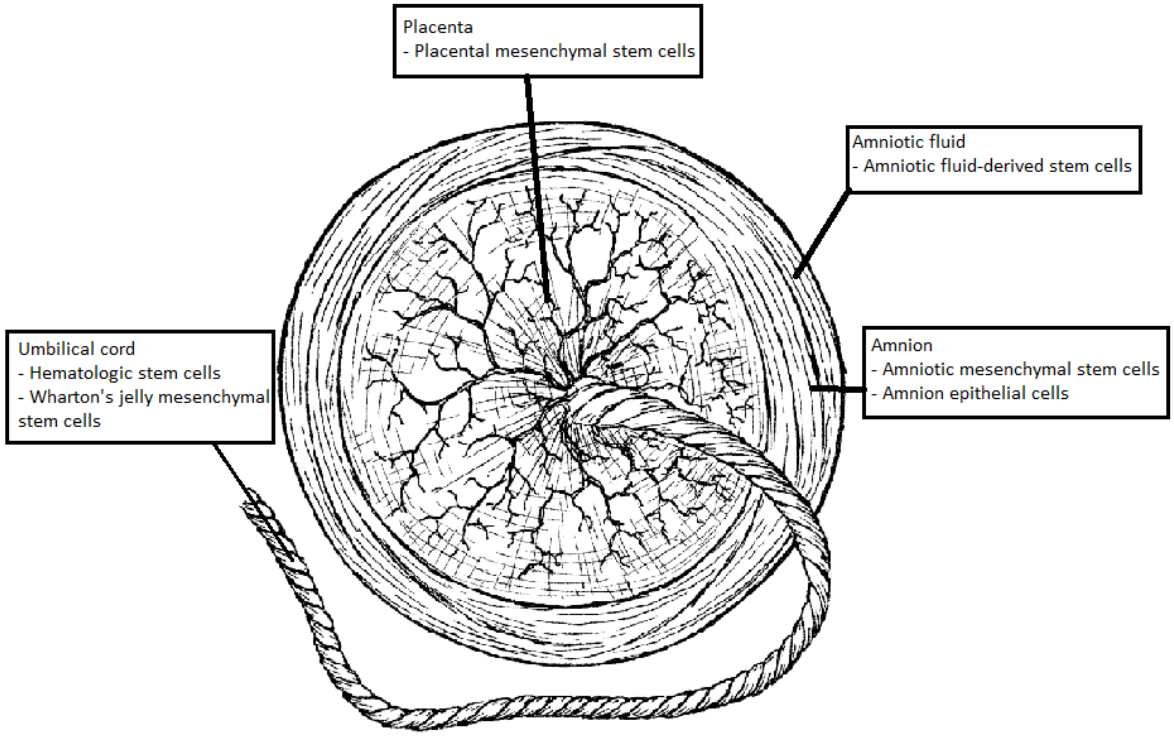

Figure 4 Different gathering possibilities for stem cells of the placenta [39]

Objectives/ Aims of the study

This thesis is part of a bigger project in which nine rounds of experiments are planned to find the best application material for AMSC, provided by the Division of cell biology, histology and embryology of the Medical University, Graz. This thesis focuses on the pilot project, in which we figured out the optimal timetable, operation technique, anaesthesia and pain management, and the first experiment. The first experimental run was set to create a baseline for the cycles to come and to have a basic oversight over the inflammation process histologically and via the blood parameters. Ultimately, these studies should be the basis for clinical trials with AMSC on chronic wounds. In this thesis we concentrate on finding the best possible application material for AMSC in wound therapy. We refer to the study by Tuca et al. 2016 and try to further mature the approach by adding more application materials and different combinations[17].

2. Methods

Cells

All human amniotic mesenchymal stem cells (=AMSC) were provided and isolated according to the protocol published by König et al. [18]. Approval of the Ethical Committee of the Medical University of Graz was granted (No. 21-079 ex 09/10).

Animals

For the animal care and for facilities suitable for our operations we cooperated with the Department for Biomedical Research of the Medical University of Graz. All experiments were approved by the ethics commission of the Animal Care and Use Committee at the Veterinary University of Vienna on behalf of the Austrian Ministry of Science and Research. (BMBWF-66.010/0047-V/3b/2018)

For the study we used 16 female mice of the species Rj:NMRI-Foxn1$^{nu/nu}$ (Janvier Labs, Le Genest-Saint-Isle, France). An autosomal mutation of the 11th chromosome leads to an aplasia of the thyme which results in an absence of t-lymphocytes[19]. Consequently, the immunodeficient mice were housed in the experimental SPF area of the Department for Biomedical Research at the Medical University of Graz.
Additionally, a side-effect of the mutation is the minder keratinization of the hair follicles which results primarily in a nude appearance of the mice. The lack of hair is the perfect basis for our study as it helps immensely with the documentation and evaluation of the wound closure.
We were able to differentiate between the mice through small hole-incisions in

their ears which code their registration number (Fig. 5).

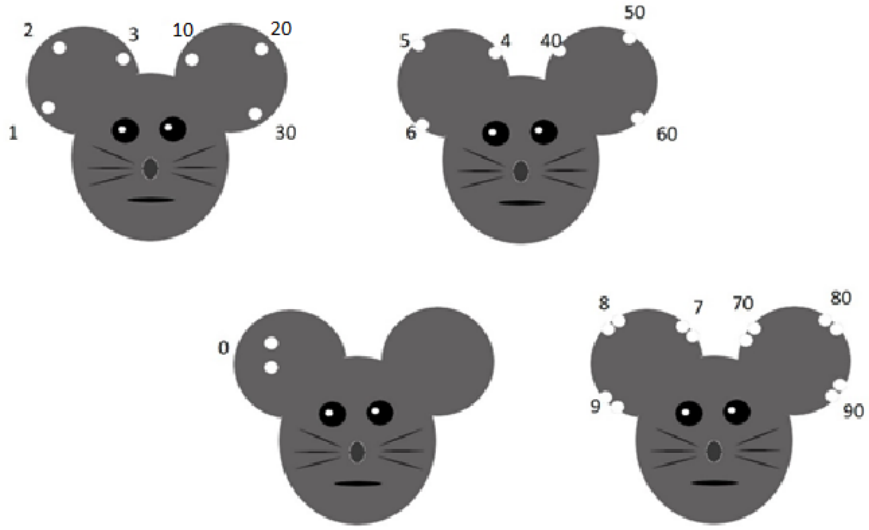

Figure 5 Schematic illustration of mouse numbering system through hole incisions

Anaesthesia and pain management

All operations and anaesthetic components were done under surveillance of a trained veterinarian or employee of the Department for Biomedical Research of the Medical University of Graz. For all our operations we used the Posi-Seal Induction chambers (Anesthesia box) for mice, rats and reptiles (Rothacher Company, Heitenried, Switzerland), which was, on the one hand, connected to the combi-vet® Base Anesthesia System Digital Flowmeter 0.3 - 16 lpm 02 (Rothacher Company, Heitenried, Switzerland) and, on the other hand, with the Fluosorber Filter Canister (Harvard Apparatus, Massachusetts, USA). This combination ensures a continuous and humified flow of the isoflurane and oxygen mixture, through an electronic flowmeter and a vaporizer. Additionally, the anaesthesia gas was absorbed immediately. The gas flow rate was 4 vol% Isoflurane and 2 - 2.5 l oxygen/minute. After approximately one minute, when the mice showed signs of a deep anaesthesia (slow and calm breathing, no movement), they were placed stomach down on a heating mat for small animals. For a clean operation field, we placed a sterile drape between the mouse and the

heating mat. To guarantee further narcosis we used an anaesthetic mask. The gas flow rate was reduced to 2 vol% with 2 - 2.5 l oxygen/minute. In order to minimize corneal dehydration, we applied Oleovit-eye gel (Fresenius Kabi Austria GmbH©, Graz, Austria). As pain management in the pilot study we used Novoalgin® 25 mg/mouse (Sanofi-Aventis Group, Paris, France) orally directly after the procedure and Nurofen® 10 mg/kg bodyweight (Reckitt Benckiser, Slough, United Kingdom) for seven days post-surgery. In the first run of the main study circle we started three days in advance with Ibuprofen 10 mg/kg and continued until three days after the operation. Additionally, the mice were shielded antibiotically with Enrofloxacin 10 mg/kg bodyweight.

Application materials

Carrier

During the experiments we focused on three materials as a carrier for the AMSC: Matrigel® (Corning, New York, USA), Matriderm® (Sorbion, Zwölfaxing, Austria) and Polycaprolactone (=PCL) and Polylactide (=PLA). In order to find the best habitat for the AMSC we used Matriderm® and PCL/PLA on their own and in different combinations with Matrigel® and a cell medium. Matrigel® is extracted from the Engelbreth- Holm-Swarm mouse sarcoma and used as a basement membrane preparation. Its main components are extracellular matrix proteins, laminin, collagen IV, nidogen-1/ entactin, and heparin proteoglycan, like perlecan. Additionally, a wide range of growth factors, including FGF, EGF, TGF beta, IGF, and PDGF, have been found. Due to its composition Matrigel® is often used to study angiogenesis in-vitro and in-vivo[20-22]. Matriderm® is a three-dimensional collagen- elastin- matrix which is clinically used to cover and promote wound healing in acute full-thickness wounds, as well as, in chronic ulcers. It is already widespread and fully integrated in clinical usage[23, 24]. The collagens are type II, III and V and it is fully biodegradable[25]. PCL/PLA is an

electro- spun scaffold made of degradable polyester. We used a PCL/PLA two-layer membrane (Institute for Multiphase Processing, Leibniz University, Germany) to simulate the structure of an epidermis. The superficial layer was close meshed (PCL100/PLA50), whereas the deeper layer was wide meshed (PCL200/PLA100). Sekula et al. 2017 have shown that through the in vitro combination of mesenchymal stem cells, collected from the human umbilical cord Wharton's jelly, with PCL/PLA have higher proliferation and migratory capabilities concerning distance and speed[26].

Plaster and wound glue

During the pilot study and another mouse trial we placed our focus on the plasters and the necessity of wound glue. Generally, we were looking for a plaster that is permeable and see through. Therefore, in the pilot study we used the transparent part of IV3000 Ported 7*9 cm (Smith and Nephew Austria, Schwechat, Austria) with three different wound glues. We compared 2-Octyl Cyanoacrylate (Dermabond®, B. Braun GesmbH Austria, Maria Enzersdorf, Austria), n-Butyl-2-Cyanoacrylate monomer (Histoacryl®, B. Braun GesmbH Austria, Maria Enzersdorf, Austria), and 2-Octyl Cyanoacrylat (Liquiband®, Advanced Medical Solutions Group plc, Winsford, Great Britain)**.** In the second trial we compared IV3000 and the Opsite Flexifix (Smith and Nephew Austria, Schwechat, Austria) in combination with physio tape.

Operation

After we placed the mice on the warming mat, we rotated them length wise by an angle of 45°. One person lifted and tightened the skin on the back of the mouse. Another person made the incision by pressing the Biopsy Punch (KAI medical, Solingen, Germany), through both skin-layers against a resistance. As resistance we used the top part of a forceps. Through this we were able to create two equal wounds exactly medially aligned. A round piece with an 8mm diameter of PCL/PLA or Matriderm® were placed in the wounds. In the pilot study, the area around the wounds was covered with glue before sealing it with IV3000. Whereas, in the follow up trial we only covered it with IV3000 (Fig.6a-f)

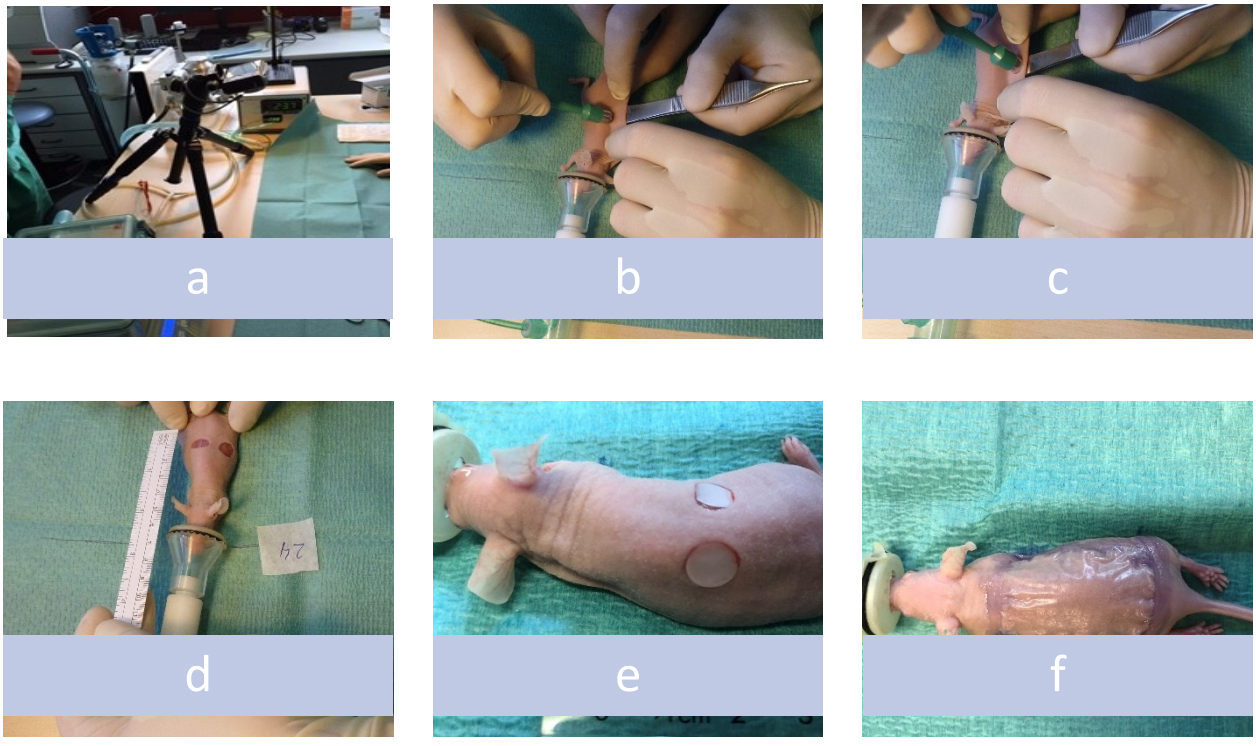

Figure 6 a- operation setup with induction chamber, camera, operating field; b&c- Mouse in anaesthesia mask during operation; d- directly after operation; e- mouse with applicated material (PCL); f- unwounded mouse with IV3000 + glue (histoacryl)

Study design

The study consisted of 2 phases: at the beginning the pilot experiment with 6 mice where all application materials are tested. Followed by one with 9 mice where we left the wounds untreated to set the baseline for experiments to come.

Pilot experiments

In the pilot study we worked with different combinations of application material, figured out the details of anaesthesia and observed macroscopic, microscopic, and blood parameters to distinguish which are worth observing and which are not. The mice had the numbers 2,4,6,8,10, and 12. The mice with the number 4 to 10 were treated with different combinations of materials (Tab. 1) and had AMSC (5x10^5 cells, pre-cultured on the carriers for 3 days in vitro) in one wound but not in the other. Whereas, the mice 2 and 12 were left untreated as a control group. We documented the current state of mice before surgery, on the 3rd, the 7th, and the 14th day by photography and weighing. On the 14th day all mice were euthanized after which we collected their blood via heart puncture and gathered the wound for histological examination.

Table 1 Application material description - pilot study

Mouse	Applicated Material Right wound	Left wound	Plaster
M 02	No wound	No wound	IV3000 + Liquiband®
M 04	PCL/PLA + Matrigel®	PCL/PLA + Matrigel® + AMSC	IV3000 + Dermabond®
M 06	Matriderm®	Matriderm® + AMSC	IV3000 + Dermabond®
M 08	PCL/PLA	PCL/PLA + AMSC	IV3000 + Histoacryl®
M 10	Matriderm® + Matrigel® + AMSC	Matriderm® + Matrigel®	IV3000 + Liquiband®
M 12	No wound	No wound	IV 3000 + Histoacryl®

First experimental run

We worked with 10 mice, labelled with the following numbers 14, 16, 18, 20, 22, 24, 26, 28, 30, and 32. As in the pilot study, we made two 8 mm punch biopsies on the back of the mice. As it is the first run of 9, we only treated it with the IV3000 plaster but no application material or stem cells. Additionally, we removed the plasters on the 3rd day to hinder the mice on removing themselves and to standardize the duration. We also documented the current state of the mice before surgery and on the 3rd, the 7th, and the 14th day by photography and weighing. In contrast to the pilot, we took blood samples every second day after the operation from the sublingual vein (Fig. 7) to gather the blood parameters continuously over the course of the wound healing process. On the 3rd, 7th, and 14th day we sacrificed three of the mice (Tab. 2) through deep sedation whereupon we collected their blood via heart puncture. Additionally, one mouse underwent sonographic examination (Tab 2.) before the surgery, on the 2nd, 6th, 9th, and 11th

day for the possibility to have a better in vivo insight on the wound healing and neovascularization process. For this we used the Vevo3100 (Visual Sonics, Japan).

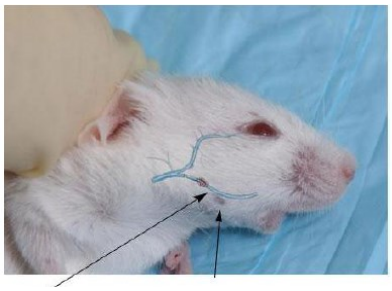

Figure 7 Illustration of the Vena sublingualis [39]

Table 2Euthanization day of the mice during first experimental run and identification of mouse used for sonographic evaluation

Mouse	Sacrification on day 3	7	14	Sonographic evaluation
M 14	X			
M 16	X			
M 18	X			
M 20		X		
M 22		X		
M 24		X		
M 26			X	
M 28			X	
M 30			X	
M 32			X	X

Data gathering

Weight and wound documentation

After the operation and on the 3rd, 7th, and 14th day we documented the wound healing process by photography. Wound healing process was analysed with the Axiovision SE64Re.4.9.1 software (Zeiss, Jena, Germany). We took the measures of the wound margin from the documentation and subsequently calculated the wound surface reduction as a percentage (Fig. 8). In the pilot study, we additionally compared the differences between treatment with AMSC and untreated wounds. After scarification, the wounds and the skin directly around the wounds were excised for histological examination. Additionally, we weighted the mice on the 3rd, 7th, and 14th day as it is a good indicator for the wellbeing of the mice.

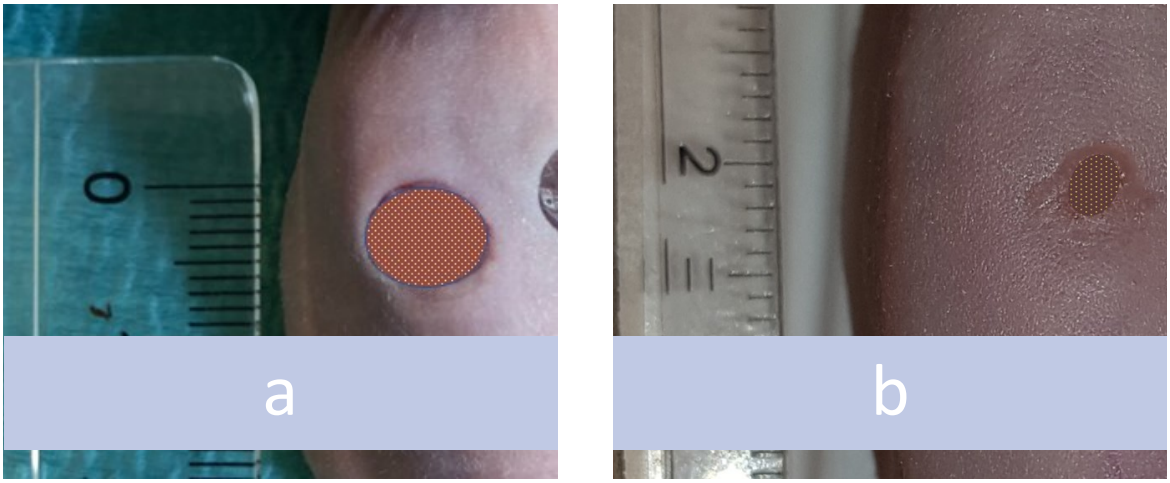

Figure 8 Schematic illustration of measurement of wounds with Axiovision SE64Re.4.9.1 software of left wound on back of mouse 4 directly after operation (a) and after 14 days (b)

Sonographic evaluation

The day before surgery we marked the operation site with the Ultrasonic Vevo3100 (Fujifilms Visualsonics, Toronto, Kanada) so the wound would not be above organ supplying vessels. Those would overshadow the wound area and falsifies the evaluation. We documented the wound ground and the epidermal thickness with its integrated measuring tools.

Blood sampling

The blood was filled either in ethylenediaminetetraacetic acid (=EDTA)- tubes or in lithium- heparin tubes. We needed a minimum of 20 µl room temperature blood for the EDTA-tubes. Whereas, for the lithium- heparin tubes we gained 75 µl of blood, which we centrifuged for 10-15 minutes with 2000 *g* to obtain plasma. This was frozen in liquid nitrogen for subsequent analysis. We gathered data concerning platelets (=PLT), platelet distribution width (=PDW), mean platelet volume (=MPV), platelet haematocrit (=PCT), erythrocytes (=RBC), haematocrit (=HCT), erythrocyte distribution width (=RDW), haemoglobin (=HGB), mean corpuscular volume (=MCV), mean corpuscular haemoglobin (=MCH), mean corpuscular haematocrit (=MCHC), white blood cells (=WBC), lymphocytes (=LYMF), monocytes (= MON) and granulocytes (=GRAN), percentage of granulocytes (=%GRAN), percentage of lymphocytes (=%LYN), and percentage of monocytes (=%MON).

Microscopic evaluation

For histological examination we needed a sample of wounds and the surrounding area. At first, we cut the skin around the wounds quadrangular (Fig. 9) and separated it from the muscle fascia with an operation scissor. Directly afterwards, the biopsies were put in formaldehyde (4%) and remained in the solution for 3

days at room temperature. As a second step, the wounds were dehydrated in a graded ethanol ladder, were cut in half, and embedded in paraffin. At last, we produced 5 serial sections every 100-200 µm from the paraffin block. The halved biopsies were placed in a way that the centre of the wounds was parallel and facing the same direction.

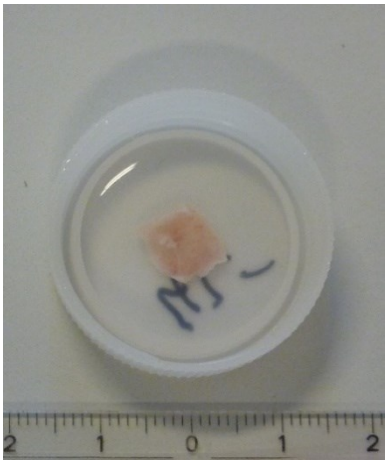

Figure 9 Biopsy of the wound with surrounding skin embedded in formaldehyde – Mouse 4 left

Haematoxylin-eosin staining

For a more specific analyzation of the wound healing and differentiation of the progression after the different days the biopsies were stained with haematoxylin-eosin. The deparaffination, rehydration, staining and final dehydration was done following the standardized protocol of the Division of Cell Biology, Histology and Embryology of the Medical University of Graz (Tab. 3). After completing the steps preparations are covered and examined under the microscope. Through this staining acidic/basophil structures like the nuclei appear blue due to the alkaline hemalaun and alkaline/acidophil structures like cytoplasm or mitochondria appear pink/red due to the Eosin. For scoring I used a Haematoxylin-Eosin assessment scoring system described by Gupta et al. [27].

Table 3Protocol for haematoxylin-eosin staining

Deparaffinization and rehydration	
Tissue Clear 1A & 1B	5 minutes each (10 total)
Tissue Clear 2A & 2B	5 minutes each (10 total)
100% EtOH/ Tissue Clear 1:1	2 minutes
100% EtOH	2 minutes
96% EtOH	2 minutes
70% EtOH	2 minutes
50% EtOH	2 minutes
Distilled Water	3 * 2 minutes

Staining	
Mayer's hemalaun	10 minutes
Distilled Water	2-3 times, until water is clear
$\boldsymbol{NH_3}$-Water	Until nuclei are blue – seconds
Distilled Water	Rinse out
Eosin 1%	1 minute
96% EtOH	2 times, until EtOH is clear
100% EtOH	2 minutes
100% ETOH/ Tissue Clear 1:1	2 minutes
Tissue Clear 2B	≥ 10 minutes
Permanent covering	Glycerol-gelatine
Drying horizontally	

Immunohistochemistry Ki-67

A few slices were selected for immunohistochemistry. We applied Ki-67 antigen with a mouse-anti-human isotope (Dako, Santa Clara, USA) with an initial concentration of 55 µg/ml and a dilution of 1:50. This immunostaining reveals nuclear reactivity in cells. The protocol was again provided by the Division of Cell Biology, Histology and Embryology of the Medical University of Graz (Tab. 4).

Table 4Protocol for immunofluorescence staining with Ki-67 antigen

Deparaffination	
Tissue Clear 1A & 1B	5 minutes each (10 total)
Tissue Clear 2A & 2B	5 minutes each (10 total)
100% EtOH/ Tissue Clear 1:1	2 minutes
100% EtOH	2 minutes
96% EtOH	2 minutes
70% EtOH	2 minutes
50% EtOH	2 minutes
Distilled Water	3* 2 minutes

Antigen retrieval	
AG Retrieval pH9 (KOS 93°C)	15 minutes
Cooling in buffer	20 minutes
Distilled Water	5 minutes

Immunofluorescence staining	
Pap Pen	Separate sections in lines
PBS (=phosphate buffered saline)	2 minutes
UV block	5 minutes
PBS	2 minutes
MOM (=mouse on mouse) blocking	60 minutes
PBS	2 minutes
Serum- free protein block	30 minutes
Primary antibody (=Mah Ki-67)	30 minutes
PBS	3* 2 minutes
Secondary antibody (=Goat anti mouse FITC (BD))	30 minutes
PBS	3* 2 minutes
Dapi	5 minutes
PBS	3*2 minutes
Permanent covering	ProLong Gold
Drying overnight, room temperature	

3. Results

Animals, anaesthesia & pain management
Pilot experiment

In the two-week period after the surgery the mice showed no signs of infections, had a good weight progress and were overall in a good condition (Figure 10(a)).

Animals, anaesthesia & pain management
First experimental run

Overall, the mice showed no signs of infection nor stress reactions in the 14th day post-surgery period. The mice showed a minimal drop in weight on the 7th day (Figure 10(b)).

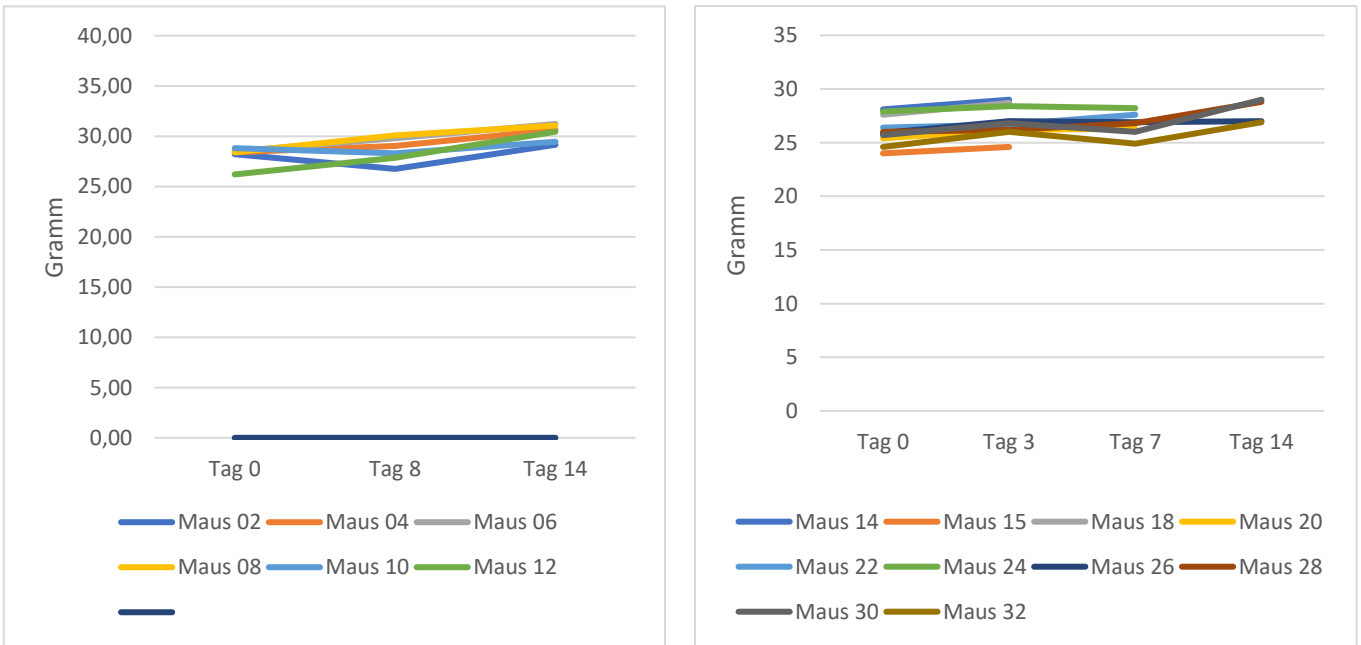

Figure 10(a- left) Pilot experiment and (b- right) First experimental run show the weight progress of the mice during the studies. During the (a) a continuous weight gain was notable whereas in (b) a small drop on the 7th day is notable.

Plaster & wound glue
Pilot experiment

Both plasters combined with Liquiband® and Histoacryl®, and one of the plasters combined with Dermabond® were detached after 3 days. After 7 days all plasters were gone (Tab. 5).

Table 5Durability of IV3000 Plaster in combination with different Wound glues

Wound-Glue	3rd day	7th day
Liquiband®	M02 detached M10 mostly detached	M10 detached
Dermabond®	M04 1/3 detached M06 unchanged	M04 & M06 detached
Histoacryl®	M08 mostly detached M12 1/3 detached	M08 & M12 detached

Plaster & wound glue
First experimental run

As we removed the plasters on the 3rd day there were no more differences in wound treatment.

Wound documentation
Pilot experiment

The difference in healing potential given through the various application combinations is noticeable through measurement of the wounds with Axiovision SE64Re.4.9.1 software (Zeiss, Jena, Germany) after 8 days. The mean wound reduction after 8 and 14 days is 57% (27% - 81%) and 97% (92% – 100%), respectively (Fig. 11 & 12).

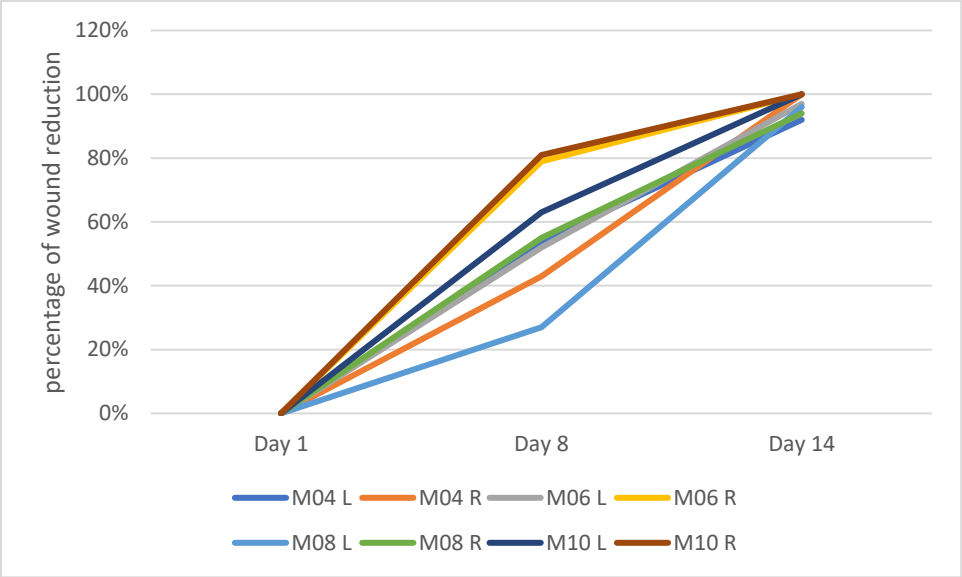

Figure 11Wound diameters 14 days postoperatively M04 L = PCL/PLA + Matrigel®; M04 R = PCL/PLA + Matrigel® + AMSC; M06 L = Matriderm® + cell medium; M06 R = Matriderm® + cell medium + AMSC; M08 L = PCL/PLA + cell medium; M08 R = PCL/PLA + cell medium + AMSC; M10 L = Matriderm® + Matrigel® + AMSC; M10 R = Matriderm®+Matrigel®

	DAY 1	DAY 3	DAY 8	DAY 14
MOUSE 04				
MOUSE 06				
MOUSE 08				
MOUSE 10			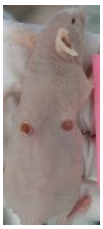	

Wound documentation
First experimental run

Measurement of the woundbet with Axiovision showed that the mean closure on the 3rd, 7th, and 14th day is 32% (-22% - 73%), 81% (51% - 97%) and 100%, respectively (Fig. 13) The number of wounds documented decreased because of the sacrification during the trial.

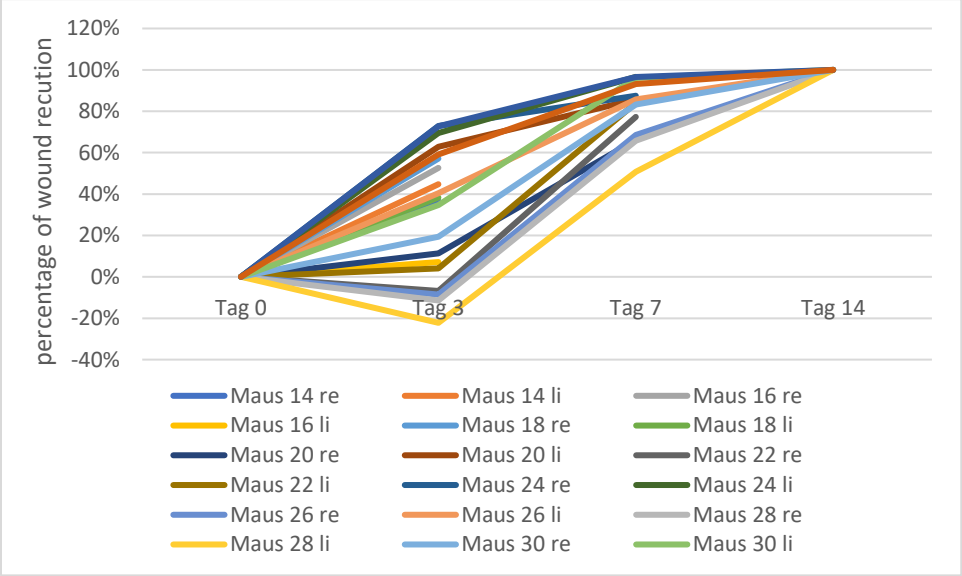

Figure 12 Diameters of all wounds 14 days postoperatively

Comparison of wound closure

Comparison of the percentual wound closure revealed that the fastest healing wounds were treated with Matriderm® + Matrigel® without AMSC (Mouse 10R), Matriderm® + cell medium with AMSC (Mouse 06R), and Matriderm® + Matrigel® with AMSC (Mouse 10L), respectively. Additionally, evaluating the haematoxylin-eosin staining with the score by Gupta et al., those wounds had full epidermal closure and at least scanty granulation tissue, moderate inflammatory infiltrate, mixed collagen fibre orientation and pattern [27]

Sonographic evaluation

The day before the surgery we measured an epidermal thickness between 0,086 – 0,105 mm (Fig. 14-a). On the first postoperative day the plaster was still attached to the mouse (Fig. 14-b), which looks similar to normal dermis on the photo, but we folded it away for a more accurate evaluation (red arrow, Fig. 14-c). The axial wound-diameter continuously decreased from day 2 (Fig. 14-c), 6 (Fig. 14-d), 9 (Fig. 13-e), 11 (Fig. 13-f) from 3,876 mm, 2,406 mm, 1,897 mm to 1,463 mm, respectively. Until the 6th day the wound penetrated through all levels of the skin. After the 9th day an epidermal layer was rebuild and the dermal wound could only be seen via ultrasonic. Transaxial the dermal wound was 3,792 mm on the 9th day and 4,473 mm on the 11th day. On the 11th day the epidermal thickness regained its baseline with 0,088 mm- 0,106 mm. On the 6th day a scab development was seen (arrow).

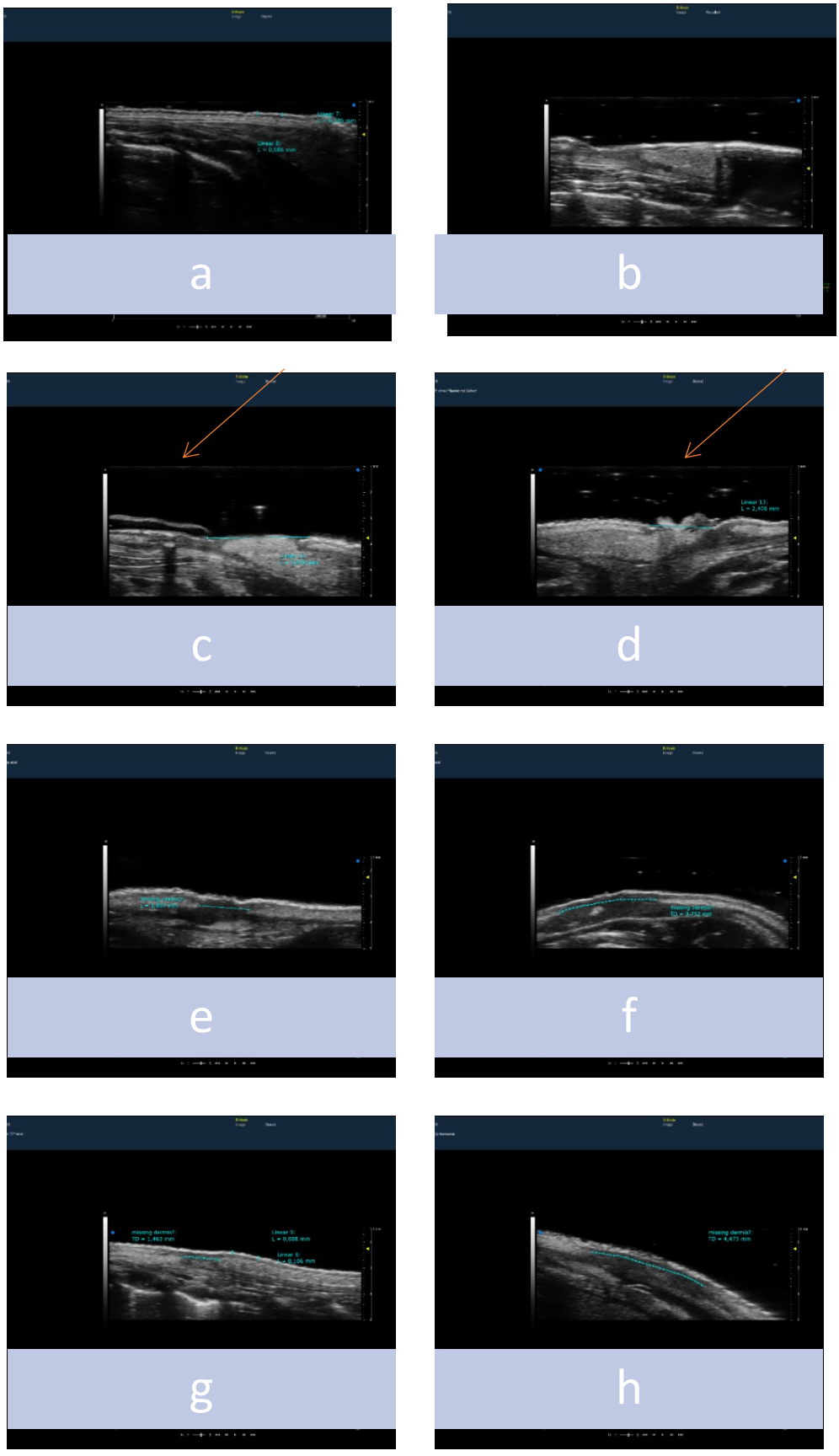

Figure 13 Ultrasonic evaluation of the wounds over time: a =day 0, b= day 1, c= day 2, d= day 6, e= day 9, f/g/h= day 11

Analysis of blood samples
Pilot experiment – wounds treated with carriers +/- AMSC

In the pilot study we only harvested the blood on the 14th day after wounding. For some parameters Janvier Labs provided the norm. Inflammation parameters white blood cells (1,22 10^9/l), lymphocytes (0,78 10^9/l), granulocytes (0,52 10^9/l), and monocytes (0,06 10^9/l) have fallen under the norm given on the 14th day (Tab. 6)

Table 6Analysis of blood-parameters on the 14th day pilot study

Parameter	Norm-Range	Unit	Mean	Minimum	Maximum
PLT	864 – 1372	10^9/l	988,33	698,00	1204
MPV		Fl	4,83	4,50	5,20
PCT		%	0,48	0,33	0,57
PDW			16,53	16,30	16,70
RBC	9,74 - 9,86	10^12/l	8,52	8,09	8,96
MCV	59-61	Fl	50,73	49,70	52,90
HCT	55-61	%	43,18	40,70	45,30
HGB	15,22 – 15,38	g/dl	12,87	12,20	13,40
MCH	15,63 - 15,77	Pg	15,05	14,80	15,70
MCHC	25 - 27	g/dl	29,75	29,30	30,10
%RDW		%	15,68	14,80	16,40
WBC	4,7 – 7,3	10^9/l	1,22	0,50	2,70
LYMF	3,16 – 5,6	10^9/l	0,78	0,30	1,60
GRAN	1 – 1,46	10^9/l	0,52	0,30	1,00
MON	0,05 – 0,09	10^9/l	0,06	0,00	0,10
%LYN		%	53,90	43,70	64,30
%GRA		%	41,14	30,90	51,20
%MON		%	4,98	4,70	5,40

Analysis of blood samples

First experimental run – untreated wounds

The blood samples were taken on the day before surgery and the 2nd, 4th, 6th, 8th, and 14th day in the first experimental run. For some parameters Janvier Labs provided the norm. In the course of the experiment it seems as if the duration of the infection lasts around 7 days. The parameters platelets (1759,34 10^9/l), white blood cells (13,37 10^9/l), lymphocytes (9,87 10^9/l), and monocytes (0,27 10^9/l) all peak on the 6th or 8th day. Granulocytes (3,37 and 3,33 10^9/l) and mean corpuscular haemoglobin (17,27 and 17,77 pg) show two peak levels on the 2nd, 7th, and 4th and 8th day, respectively (Fig. 15, Tab. 7).

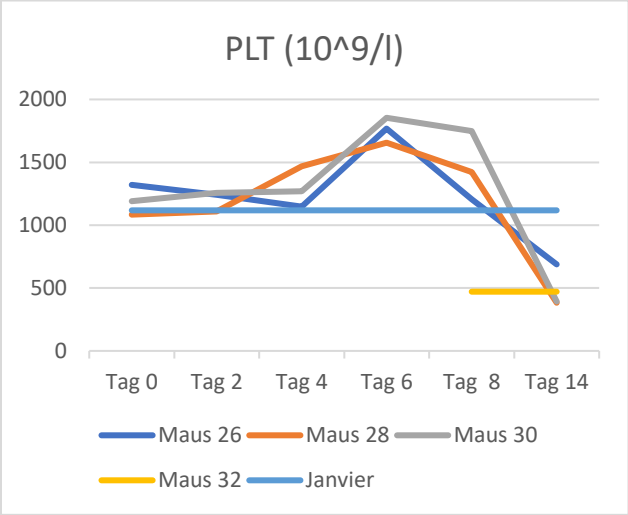

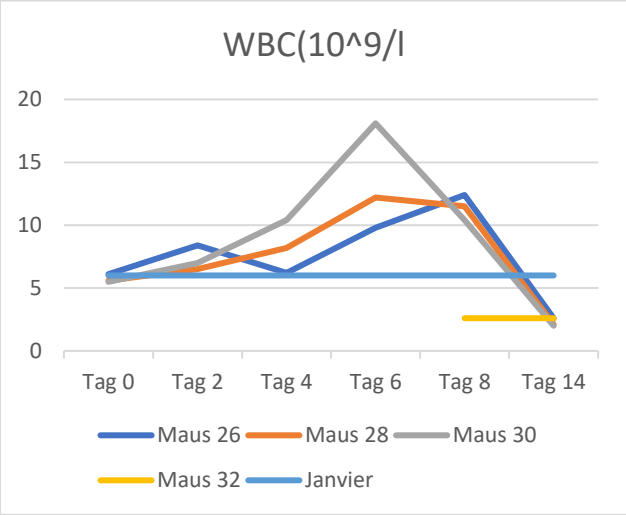

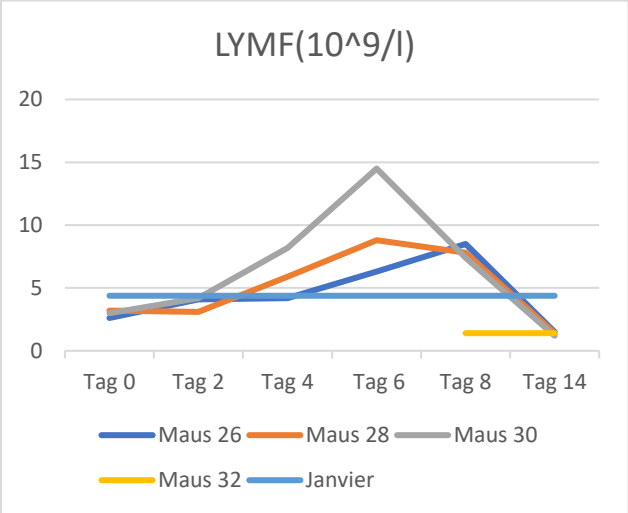

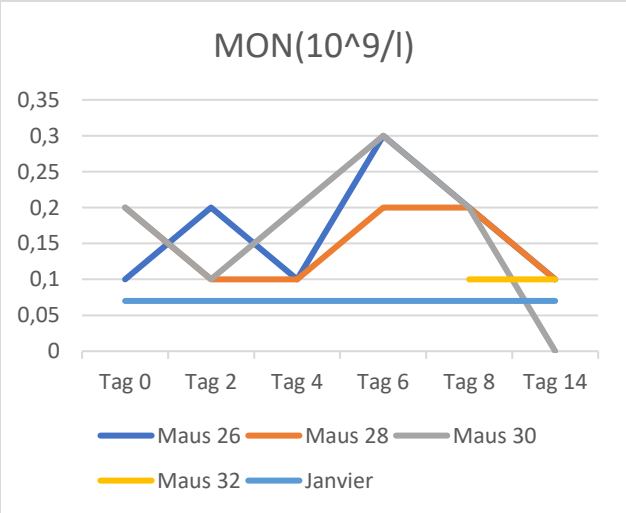

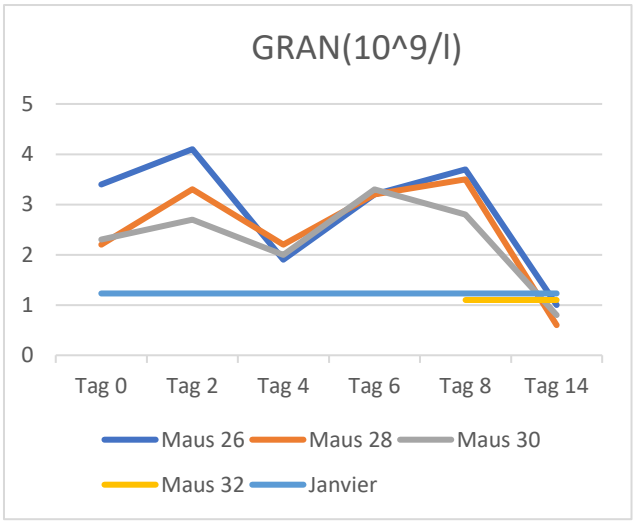

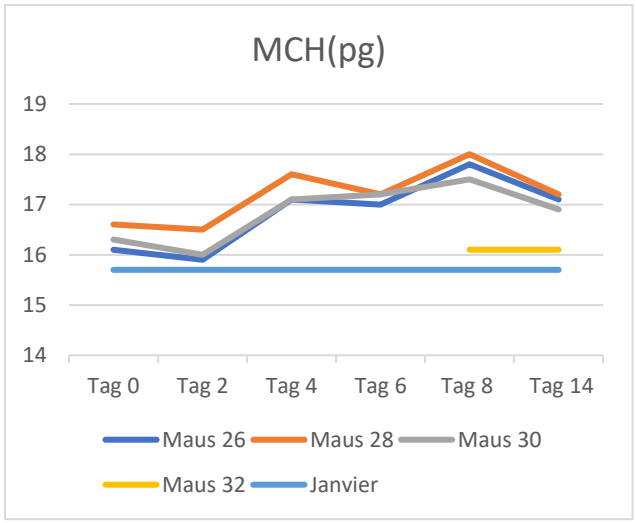

Figure 14 course of the blood parameters platelets (=PLT), white blood cells (=WBC), lymphocytes (=LYMF), monocytes (=MON), granulocytes (=GRAN) and mean corpuscular haemoglobin (MCH) during the first experimental run showing the different peaks- PLT, WBC, LYMF, MON between the 6th or 8th day, GRAN on the 6th and 8th day, and MCH on the 4th and 8th day

Table 7Analysis of blood parameters of Mice 26-32 with given norm by Janvier Labs and calculated mean, minimum and maximum in brackets; we only collected data of mouse 32 on day 14

Parameter	Norm-Range	Unit	Day 0	Day 2	Day 4	Day 6	Day 8	Day 14
PLT	864 – 1372	10^9/l	1016,75 (1085-1320)	1202,00 (1108 – 1257)	1295,67 (1148 – 1469)	1759,34 (1656 – 1854)	1459,34 (1206 – 1749)	483,75 (383 – 688)
MPV		Fl	4,77 (4,60 – 4,90)	4,47 (4,30 – 4,70)	4,67 (4,60 – 4,80)	4,63 (4,50 – 4,80)	4,70 (4,30 – 5,10)	5,18 (4,80 – 5,30)
PCT		%	0,57 (0,53 – 0,63)	0,54 (0,52 – 0,55)	0,60 (0,55 – 0,68)		0,64 (0,61 – 0,67)	0,25 (0,20 – 0,36)
PDW			16,60 (16,30 – 16,80)	16,37 (16,20 – 16,20)	16,70 (16,50 – 16,90)	16,60 (16,50 – 16,70)	17,00 (16,30 – 17,70)	17,00 (16,50 – 17,40)
RBC	9,74 - 9,86	10^12/l	9,53 (9,12 – 9,77)	8,89 (8,18 – 9,32)	9,04 (8,48 – 9,59)	8,44 (7,81 – 9,22)	8,57 (8,21 – 8,91)	7,25 (5,69 – 8,40)
MCV	59-61	Fl	50,63 (50,00 – 51,30)	51, 07 (49,70 – 52,00)	50,37 (50,00 – 51,10)	52,00 (51,20 – 52,70)	52,30 (51,90 – 52,60)	50,78 (47,70 – 52,50)
HCT	55-61	%	48,20 (46,70 – 49,4)	45,30 (42,50 – 47,90)	45,47 (43,30 – 47,90)	43,80 (40,60 – 47,20)	44,73 (43,10 – 46,20)	36,63 (29,80 – 43,40)
HGB	15,22 – 15,38	g/dl	15,63 (15,20 – 15,90)	14,37 (13,50 – 14,90)	15,63 (15,00 – 16,40)	14,50 (13,50 – 15,70)	15,27 (14,80 – 15,90)	12,20 (9,80 – 14,40)
MCH	15,63 - 15,77	Pg	16,33 (15,90 – 16,60)	16,13 (15,90 – 16,60)	17,27 (17,10 – 17,60)	17,13 (17,00 – 17,20)	17,77 (17,50 – 18,00)	16,83 (16,90 – 17,20)

MCHC	25 - 27	g/dl	32,37 (31,90 – 32,70)	31,70 (31,10 – 32,30)	34,33 (34,20 – 34,60)	33,03 (32,70 – 33,20)	34,10 (33,60 – 34,40)	33,23 (32,80 – 33,90)
%RDW		%	13,90 (13,10 – 15,10)	14,50 (13,90 – 14,90)	14,10 (13,70 – 14,50)	16,43 (15,40 – 17,50)	16,27 (15,40 – 16,70)	15,50 (14,30 – 16,10)
WBC	4,7 – 7,3	10^9/l	5,73 (5,60 – 6,10)	7,30 (6,50 – 8,40)	8,27 (6,20 – 10,40)	13,37 (9,80 – 18,10)	11,43 (10,40 – 12,40)	2,33 (2,00 – 2,620)
LYMF	3,16 – 5,6	10^9/l	2,93 (2,60 – 3,20)	3,80 (3,10 – 4,20)	6,10 (4,20 – 8,20)	9,87 (6,30 – 14,50)	7,90 (7,40 – 8,50)	1,38 (1,20 – 1,50)
GRAN	1 – 1,46	10^9/l	2,63 (2,20 – 3,40)	3,37 (2,70 – 4,10)	2,03 (1,90 – 2,20)	3,23 (3,20 – 3,30)	3,33 (2,80 – 3,70)	0,88 (0,60 – 1,10)
MON	0,05 – 0,09	10^9/l	0,17 (0,10 – 0,20)	0,13 (0,10 – 0,20)	0,13 (0,10 – 0,20)	0,27 (0,20 – 0,30)	0,20 (0,20 – 0,20)	0,08 (0,00 – 0,10)
%LYN		%	51,77 (42,20 – 57,80)	52,00 (47,20 – 60,00)	72,53 (64,70 – 80,10)	72,33 (64,70 – 80,10)	69,10 (67,50 – 71,30)	60,15 (55,20 – 68,80)
%GRA		%	45,10 (38,80 – 55,00)	45,87 (38,10 – 50,90)	25,53 (19,50 – 30,30)	25,50 (18,00 – 32,50)	29,17 (26,90 – 30,80)	36,20 (27,00 – 41,20)
%MON		%	3,13 (2,80 – 3,40)	2,13 (1,90 – 2,60)	1,93 (1,80 – 2,00)	2,17 (1,80 – 2,80)	1,73 (1,70 – 1,80)	3,65 (2,60 – 4,20)

Comparisson of blood samples after 14 days- Pilot study – First experimental run

Granulocytes had a peak on the 2nd and 8th day. A comparison of the 14th day blood samples (Fig. 16) shows that the amount of white blood cells, lymphocytes, and granulocytes in the pilot study (wounds treated with carrier +/-AMSC) is lower than in the first experimental run (untreated wounds). Only white blood cells with the combination of Matriderm® with AMSC were higher than in the untreated control group. Some blood samples could not be fully analyzed (MON- M8, M10, M12, M30; GRAN- M8, LYMF- M8).

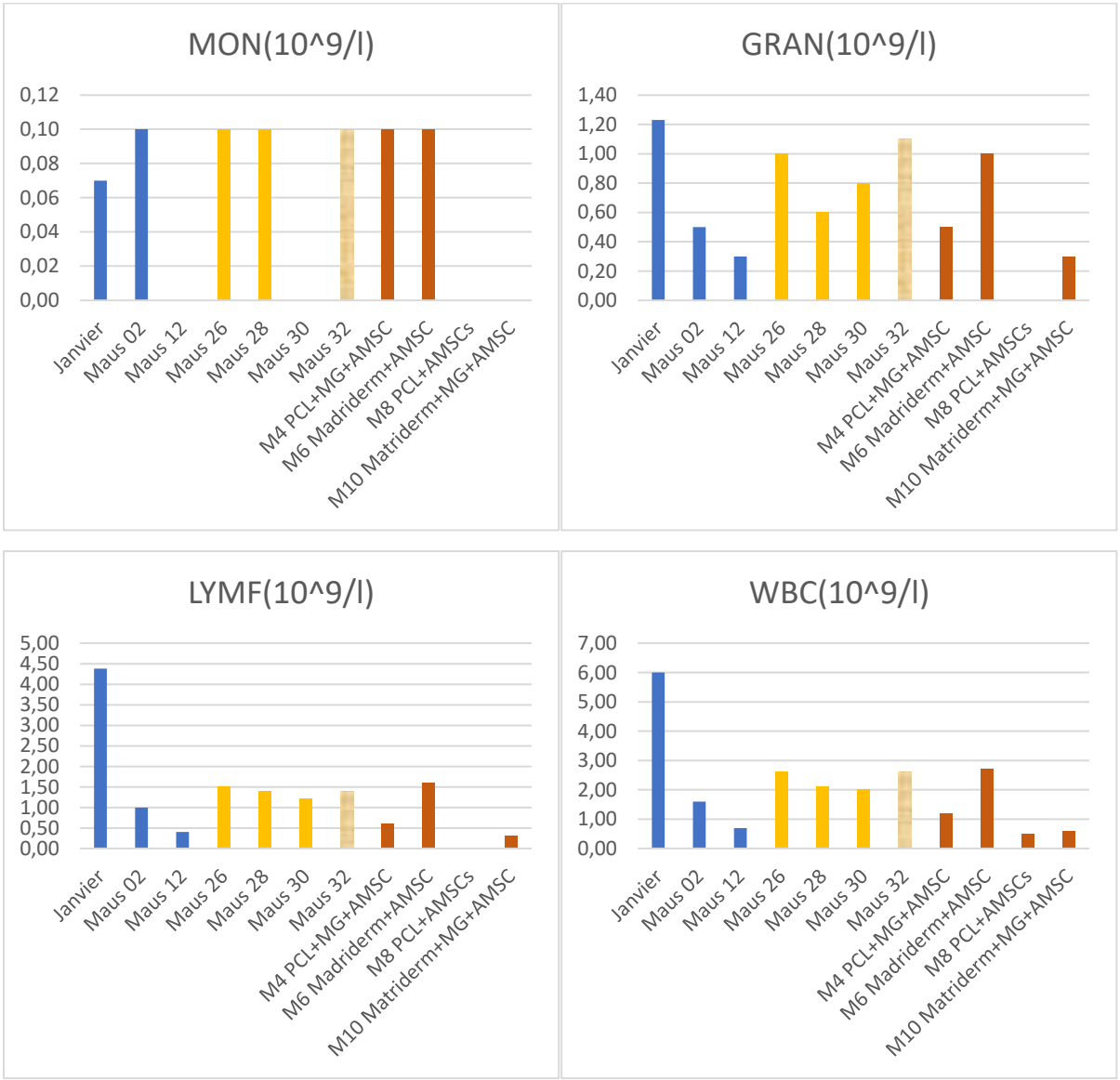

Figure 15 Comparison of white blood cells, lymphocytes, granulocytes, and monocytes on 14th day of pilot study (brown bars) and first experimental run (Mice 26-32); Janvier gave their norm and Mouse 02 was uninjured

Microscopic evaluation
Pilot experiment

After 14 days nearly all wounds regained full closure. The regeneration proceeds from the border of the wounds. Some already form new sebaceous glands and hair follicles. Wounds treated with AMSC have, compared to their counterpart, mostly a more advanced epidermal keratinization and a better organization of the collagen fibres (Tab. 8).
We were able to find traces of evidence in the epidermal and dermal layers of Matriderm® and Matrigel® in the slices stained with H.E. Cells of the connective tissue seem to migrate into Matriderm®. Even though, it was not possible to record nuclear reactivity with the Ki-67 staining and the FITC filter, we found unspecific autofluorescence of PCL/PLA detected with the TRITC filter (Fig. 17). Additionally, they seem to be integrated into the wound area without causing any inflammation signs.

Table 8Comparison of wounds with HE- staining after 14 days and scored with the score published by Gupta et al[27]

MOUSE + SIDE	MICROSCOPIC PICTURE	ENLARGED	ASSESSMENT
MOUSE 04 LEFT =PCL/PLA + MATRIGEL®	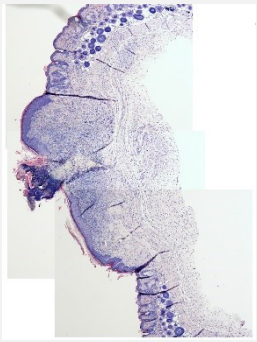	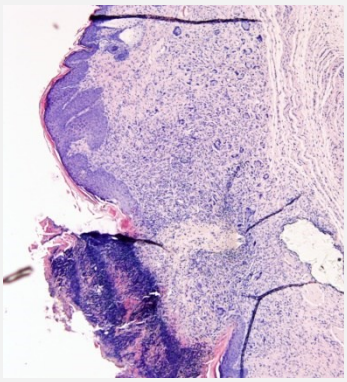	No epidermal closure Profound granulation tissue Plenty inflammatory infiltrate Mixed collagen fibre orientation and pattern
MOUSE 04 RIGHT = PCL/PLA + MATRIGEL® + AMSC	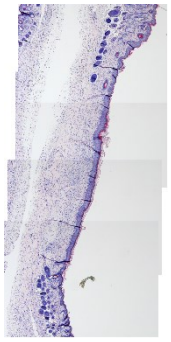	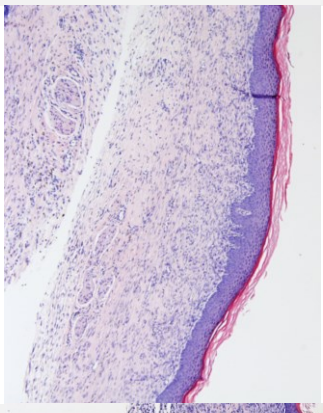	Full epidermal closure Scanty granulation tissue A few inflammatory infiltrate Horizontal collagen fibre orientation and fascicular pattern
MOUSE 06 LEFT = MATRIDERM® + CELL MEDIUM	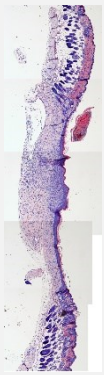	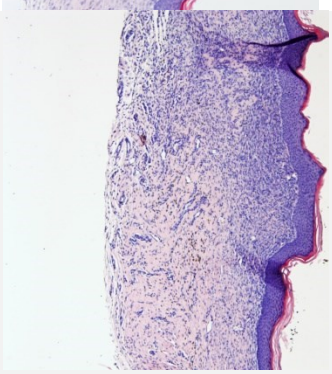	Full epidermal closure Scanty granulation tissue Moderate inflammatory infiltrate Mixed collagen fibre orientation and pattern
MOUSE 06 RIGHT = MATRIDERM® + CELL MEDIUM + AMSC	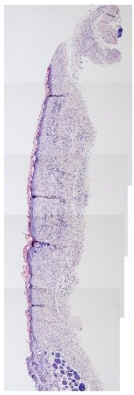	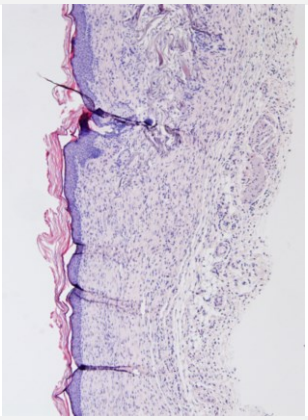	Full epidermal closure Absent granulation tissue A few inflammatory infiltrate Horizontal collagen fibre orientation and fascicular pattern

MOUSE 08 LEFT =PCL/PLA + CELL MEDIUM	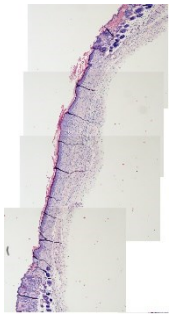	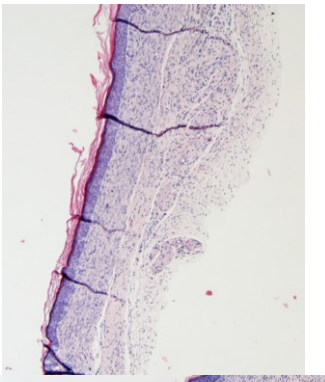	Full epidermal closure Absent granulation tissue A few inflammatory infiltrate Horizontal collagen fibre orientation and fascicular pattern
MOUSE 08 RIGHT =PCL/PLA + CELL MEDIUM + AMSC	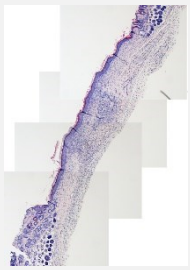	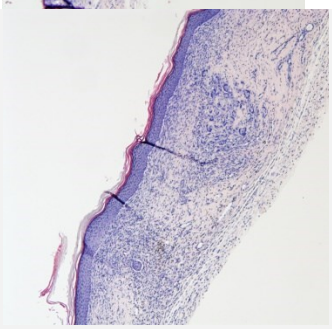	Full epidermal closure Scanty granulation tissue Moderate inflammatory infiltrate Mixed collagen fibre orientation and pattern
MOUSE 10 LEFT = MATRIDERM® + MATRIGEL® + AMSC	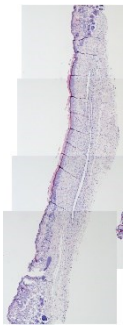	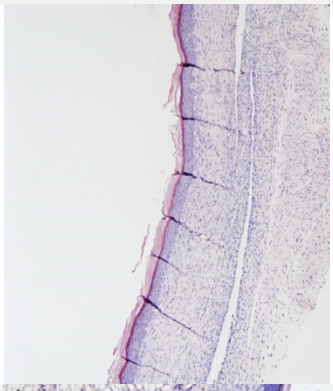	Full epidermal closure Absent granulation tissue A few inflammatory infiltrate Horizontal collagen fibre orientation and fascicular pattern
MOUSE 10 RIGHT = MATRIDERM® + MATRIGEL®	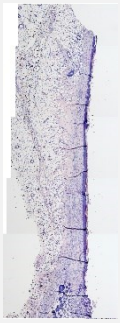	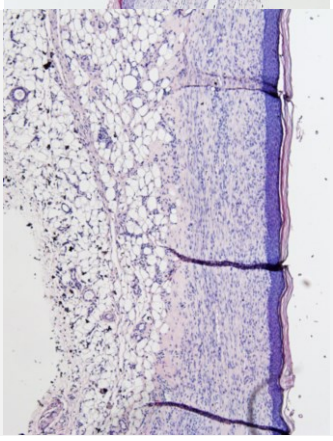	Full epidermal closure Scanty granulation tissue Moderate inflammatory infiltrate Mixed collagen fibre orientation and pattern

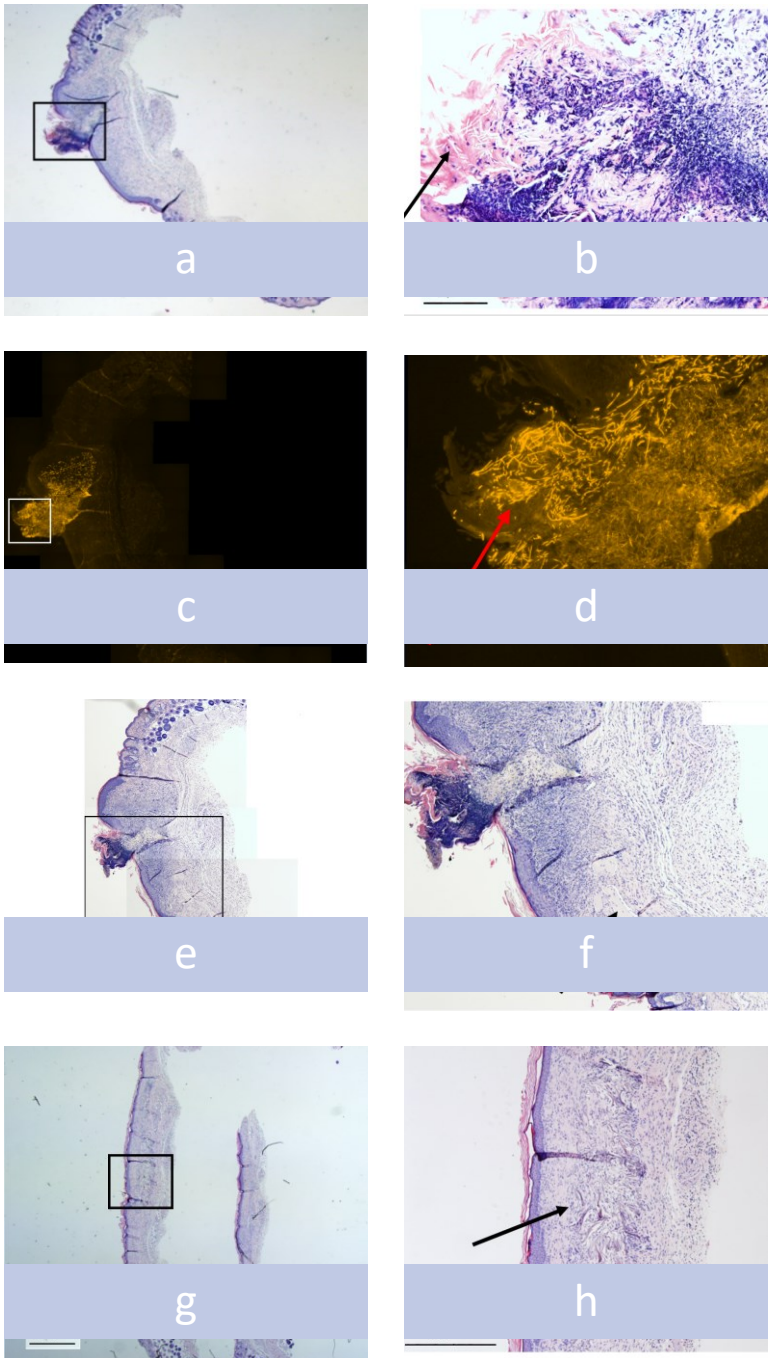

Figure 16 A list of different pictures of slices of the wounds. The left column depicts an overview of the wound and the square indicates the correlating enlarged area of the right column. ‘a’ and ‘b’ are the left wound of mouse 4 where you can see remnants PCL/PLA (arrow), wound crust (purple), stratum corneum (red). ‘c’ and ‘d’ is the same wound stained with Ki-67, though which the high fluorescence with Cy3 of PCL/PLA appears. ’e’ and ‘f’ show the right wound, mouse 4, where we found Matrigel®, which seems to be capsuled (arrow), high amounts of fibroblasts, excessive collagen fibres and thickened epidermal layer. ‘g’ and ‘f’ are pictures of the right wound, mouse 6. We identified loosened Matriderm® (arrow) with infiltrated fibroblasts, less collagen fibres and a better organization of the connective tissue than the wounds of mouse 4.

4. Discussion

Differences in wound closure of mice and men

As mice are easy to control, easy to standardize and their price to performance ratio is good they are the most often used animal model. Nevertheless, there are some major differences between mouse and human skin structures. Human skin is (100µm) thicker, has more layers (5 to 10), subcutaneous tissue differs depending on site, age, sex, and nutrition in both[28]. Further, the pure existence of panniculus carnosus in mice changes the wound healing completely. It is an additional muscle layer under the adipose tissue from which the wound contraction appears in mice wound healing[29]. Consequently, developing strategies to make wound healing of mice and men more comparable is in great focus. Beside genetically modified models, humanized models, adapted wound models are the most common. For example, the splinted model, which is described by Galiano, et al. 2004, uses a silicon ring that is fixated around the wound to prevent wound contracture and the analyzation all phases wound healing[30]. Despite the differences between human and mouse wound healing we decided on not manipulating the wound contracture because we feared that the additional incisions, which would be required to fixate the silicon ring, would change the inflammation markers and our matrices would be stiff enough to be a counterpart to the contraction.

Influence of wound glue

In the pilot study we used Liquiband®, Dermabond® and Histoacryl® as a fixation for the plasters as wound glues are an omnipresent alternative or addition in surgery in present days. Studies have shown that closing the operation site with glues has no disadvantage compared to sutures in healing time, inflammation or scar formation[31, 32]. Whereas, Chen, et al. 2017 found an association between a reduced activity of stem cells in wounds closed with 2-octylcynoacrylate (=Dermabond®). Their results suggest that direct contact of the MSCs with the glue lead to a decreased metabolic activity and direct or indirect contact hinders the secretion of growth hormones[33]. In our study, we quickly realized that the glue will not reduce neither the manipulation by the mice nor prolongs the durability of the plaster. Consequently, we decided to discard extra fixation and decided to remove the plasters on the third day.

Application material

We were able to find evidence of Matriderm®, Matrigel® and PCL/PLA in the wounds. All three materials show good integration into the wound-side and seem to dissolve without delay. In comparison to the other two materials, the wound treated with PCL/PLA showed an accumulation of cells. It gets resorbed slowly through hydrolytic degradation[34]. Furthermore, the fact that we were not able to detect specific staining of Ki-67 with the FITC filter leads to the conclusion that no living human cells are present after 14 days in the wounds. The result are coherent with a study by Tuca, et al. 2016[17] in which they compared the influence of Matrigel® +/- AMSC and Matriderm® +/- AMSC on wound healing. After, many studies have already proven that Matriderm® favours skin recovery[17, 24] Matrigel® seems to be the component that accelerates it even

more. Recently, PCL/PLA got more and more attention due to the fact that cell viability, proliferation, migratory capabilities and angiogenic differentiation potential are promoted when seeded in PCL/PLA membranes[26, 34]. The wound we treated with PCL/PLA did not show an accelerated healing tendency. Nevertheless, the wound covered with PCL/PLA + Matrigel® and AMSC, did show a further progressed healing in the haematoxylin- eosin stained. Consequently, combining the advantages of PCL/PLA, as excellent cell base, and Matrigel®, as ideal cell medium, show promising results as wound treatment.

Pilot study:

The results of the pilot study, and especially in comparison with the first experimental run, indicates that Matriderm® in combination with or without Matrigel and AMSC has the best healing tendencies. Those results are supported by the bachelor theses of Hochwimmer and Neumaier written and conducted at the Division of Cell biology, Histology and Embryology of the Medical University, Graz. Hochwimmer and Neumaier used slices of the same mice stained with anti-CD31 antigen, and Masson Trichrom straining, respectively. Anti-CD31 marks to young and matured endothelial cells, which in this case are present in the newly formed capillaries. Due to the Masson Trichrom staining collagen colours blue, which can be seen as a sign for maturation in wounds. In both theses, Matriderm® with or without Matrigel and AMSC, had the highest amount of collagen and the highest number of newly formed capillaries. Interestingly, wounds treated with PCL/PLA were nearly as good capilarized as the ones treated with Matriderm®[35, 36].

First experimental run

The first experimental run was conducted without any application material. It is thought to set the baseline for the following to come. The wound- closure on the 7th day was on average 81% and 100% on the 14th day. Compared to the pilot study the re-epithelialization on the 7th day was further progressed. The missing of carrier substances, which have a certain degree of firmness to withhold skin contraction, might be the reason for this outcome.
The ultrasonic evaluation of the wound beds was primarily thought as an alternative possibility to measure neoangiogenesis. Unfortunately, this was not possible. However, given the fact, that it was possible to quantify healing tendencies without euthanisation a mouse might be a chance of reducing animals needed in studies to come.

Comparison of blood samples after 14 days - pilot study and first experimental run:

This was done in order to track the chronological sequence of blood-cells, inflammation parameters and associate the findings with healing tendencies and to set a reference to the norms given by Janvir Labs. The first peak could be because of the initial recruitment after wounding. The 2nd on the 8th day, as the peak of white blood cells, lymphocytes, monocytes, and thrombocytes may be because we stopped administering ibuprofen.

Due to the small amount of mice statistical testing is not possible so far.

5. Conclusio and Outlook

Our results suggest confirmation of an accelerated wound healing and re-epithelization through the combination of Matriderm® + Matrigel® with or without AMSC. Additionally, PCL/PLA + Matrigel® seems to be an equivalent and maybe a cheaper alternative as it had the same histological outcome. Moreover, testing the blood on inflammation markers might give more insight into the impact MSC have on wound healing locally and systemically. Further, it should be considered to extend the parameters for a clearer picture.

Appendix: Protocols of pilot study and first experimental run

Usage of Stem Cells in Woundhealing II:

Rj:NMRI-Foxn1nu/Foxn1nu – Janvier

Gender: ♀

Mousenumber:_____ _____

Date of Birth:

Applicationmaterial:

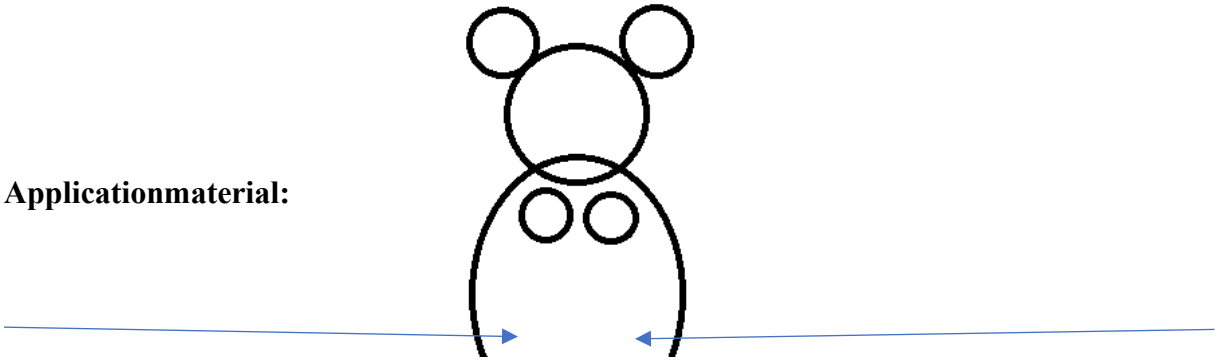

Day 0 - Date: _____

- **Weight**: _____g
- **Foto**: □
- **Bloodsampling**: □
- **In-vivo-Imaging:** □
- **Ultrasonic:** □
- **Complications?** Yes □ No □

  If yes which?

Day 3 - Date: _____

- **Weight**: _____g
- **Foto**: □
- **Bloodsampling**:
- **In-vivo-Imaging:** □

- **Ultrasonic:** □
- **Biopsie:** □
- **Complications?** Yes □ No □

  If yes which?

Mousenumber:_____

Day 7 - Date: _____

- **Weight**: _____g
- **Foto**: □
- **Bloodsampling**:
- **In-vivo-Imaging:** □
- **Ultrasonic:** □
- **Biopsie:** □
- **Complications?** Yes □ No □

  If yes which?

Day 14 - Date: _____

- **Weight**: _____g
- **Foto**: □
- **Bloodsampling**:
- **In-vivo-Imaging:** □
- **Ultrasonic:** □
- **Biopsie:** □
- **Complications?** Yes □ No □

  If yes which?

Comments

References:

1. Sorg, H., et al., *Skin Wound Healing: An Update on the Current Knowledge and Concepts.* European Surgical Research 2017, 2016. **58**: p. 81-94.
2. Lippert, H., *Wundatlas - Kompendium der komplexen Wundbehandlung* 3ed. 2012, Stuttgard, New York: Thieme.
3. Lindholm, C. and R. Searle, *Wound management for the 21st century: combining effectiveness and efficiency.* International Wound Journal, 2016. **13**: p. 5-15.
4. Austria, S., *Lebenserwartung ohne chronische Krankheit seit 2003*. 2019, Bundesanstalt Statistik: [cited 06.05.2020], available at http://www.stat.at/web_de/statistiken/menschen_und_gesellschaft/gesundheit/gesundheitszustand/lebenserwartung_in_gesundheit/041833.html.
5. Robine, J. and E. Camboi *Healthy Life Expactancy in Europe*. Population & Societies, 2013. **499**, 1-4.
6. Childs, D.R. and A.S. Murthy, *Overview of Wound Healing and Management.* Surgical Clinics of North America, 2017. **97**: p. 189-207.
7. Lüllmann-Rauch, R. and F. Paulsen, *Taschenlehrbuch Histologie*. Vol. 4. 2012: Georg Thieme Verlag KG.
8. Prodinger, C.M., et al., *Current and Future Perspectives of Stem Cell Therapy in Dermatology.* Annals of Dermatology, 2017. **29**: p. 667-687.
9. Hu, M.S., et al. *Mesenchymal Stromal Cells and Cutaneous Wound Healing: A Comprehensive Review of the Background, Role, and Therapeutic Potential*. Stem Cells International, 2018. **2018**, 13 DOI: 10.1155/2018/6901983.
10. Dominici, M., et al., *Minimal criteria for defining multipotent mesenchymal stromal cells. The International Society for Cellular Therapy position statement.* International Society for Cellular Therapy, 2006. **8**: p. 315-317.
11. Crisan, M., et al., *A Perivascular Origin for Mesenchymal Stem Cells in Mulitple Human Organs.* Cell Stem Cell, 2008. **3**: p. 301-313.
12. Kanji, S. and H. Das *Advances of Stem Cell Therapeutics in Cutaneous Wound Healing and Regeneration*. Mediators of Inflammation, 2017. **2017**, 14 DOI: 10.1155/2017/5217967.
13. Farhadihosseinabadi, B., et al. *Amniotic membrane and its epithelial and mesenchymal stem cells as an appropriate source for skin tissue engineering and regenerative medicine*. Artificial Cells, Nanomedicine, and Biotechnology, 2018. 11 DOI: 10.1080/21691401.2018.1458730.
14. Davis, J.S., *II. Skin Grafting at the Johns Hopkins Hospital.* Annals of Surgery, 1909. **50**: p. 542-549.
15. De Rotth, A., *Plastic Repair of Conjunctival Defects with Fetal Membranes.* JAMA Ophthalmology, 1940. **23**: p. 522-525.

16. Dua, H.S., et al., *The Amniotic Membrane in Ophthalmology.* Survery of Ophtalmology, 2004. **49**: p. 51-77.
17. Tuca, A.C., et al., *Comparison of Matrigel and Matriderm as a carrier for human amnion-derived mesenchymal stem cells in wound healing.* Placenta, 2016. **48**: p. 99-103.
18. Konig, J., et al., *Amnion-derived mesenchymal stromal cells show angiogenic properties but resist differentiation into mature endothelial cells*, in *Stem Cells Dev*. 2012. p. 1309-20.
19. Janvier Labs, RESEARCH-MODEL-NMRI NU,[cited 13.10.2020], available at https://www.janvier-labs.com/rodent-research-models-services/research-models/per-species/mutant-mice/product/nmri-nu.html.
20. Incorporated, C. and L. Sciences, *Corning® Matrigel® Basement Membrane, Matrix for 3D Culture In Vitro*, [cited 23.09.19], available at *https://www.corning.com/catalog/cls/documents/application-notes/Application_Note_CLS-DL-AN 414_Matrigel_Matrix_3D_In_Vitro_Protocol.pdf*, Cornig, Editor. 2017, Corning Incorporated. p. 2.
21. Gabriel Benton, I.A., Jay George, Hynda K. Kleinman, Jennifer Koblinski, *Matrigel: From discovery and ECM mimicry to assays and models for cancer research.* Elsevier, 2014. **79-80**: p. 3-18.
22. Kastana, P., et al., *Matrigel Plug Assay for In Vivo Evaluation of Angiogenesis.* The Extracellular Matrix: Methods and Protocols, Methods in Molecular Biology, 2019. **1952**: p. 219-232.
23. Tchero, H., et al., *Failure rates of artificial dermis products in treatment of diabetic foot ulcer: A systematic review and network meta-analysis*. 2017: Wound repair and regeneration. p. 25.
24. Petersen, W., et al. *The use of collagen-based matrices in the treatment of full-thickness wounds*. 2016.
25. Sorbion Austria GmBH, *Matriderm®* [cited 03.04.2020], available at w*ww.sorbionaustria.at/vortraege*
26. Sekuła, M., et al., *Polylactide- and polycaprolactone-based substrates enhance angiogenic potential of human umbilical cord-derived mesenchymal stem cells in vitro - implications for cardiovascular repair.* Materials, Science and Engineering, 2017. **77**: p. 521-533.
27. Gupta, A. and P. Kumar, *Assessment of the histological state of the healing wound.* Plastic and Aesthetic Research, 2015. **2**(5): p. 239-242.
28. Zomer, H.D. and A.G. Trentin, *Skin wound healing in humans and mice: Challenges in translational research.* Journal of Dermatological Science, 2018. **90**: p. 3-12.

29. Gerber, P.A., B.A. Buhren, and H.H. Schrumpf, B. Zlotnik, A. Hevezi, P., *The top skin-associated genes: a comparative analysis of human and mouse skin transcriptomes.* Biological Chemistry, 2014. **395**: p. 577-591.

30. Galiano, R.D., et al., *Quantitative and reproducible murine model of excisional wound healing.* Wound Repair and Regeneration, 2004. **12**: p. 485-492.

31. Jan, H., et al., *LiquiBand® Surgical S topical adhesive versus sutures for the closure of laparoscopic wounds. A randomized controlled trial.* Gynecological Surgery, 2013. **10**: p. 247-252.

32. Koonce, S.L., et al., *A Prospective Randomized Controlled Trial Comparing N-butyl-2 Cyanoacrylate (Histoacryl), Octyl Cyanoacrylate (Dermabond), and Subcuticular Suture for Closure of Surgical Incisions.* Annals of Plastic Surgery, 2015. **74**: p. 107-110.

33. Chen, Y.J., et al., *Effect of 2-octylcyanoacrylate on placenta derived mesenchymal stromal cells on extracellular matrix.* Placenta, 2017. **59**: p. 163-168.

34. Woodruff, M.A. and D.W. Hutmacher, *The return of a forgotten polymer-Polycaprolactone in the 21st century.* Progress in Polymer Science, 2010. **35**: p. 1217-1256.

35. Hochwimmer, A.-T., *Histologische Analyse der Neovaskularisierung in der Wundheilung nach Applikation von mesenchymalen Stammzelen der humanen Plazenta*, [Bachelorthesis]*, Medical University Graz*. 2019.

36. Neumaier, S., *Histologische Analyse der Kollagensekretion in der Wundheilung nach Applikation von mesenchymalen Stammzellen der humanen Plazenta* [Bachelorthesis], 2020, Medical University Graz.

Image directory:

37. Figure 1: [cited 08.08.2020]
Wound healing phases, available at:
https://commons.wikimedia.org/wiki/File:Wound_healing_phases.png
38. Figure 3: [cited 08.08.2020]
Schematic Stem Cell Pedigree, adapted from:
https://commons.wikimedia.org/wiki/File:Figure_2._R%C3%A9sultats_de_diff%C3%A9renciation_de_cellules_souches_en_une_des_trois_diff%C3%A9rentes_cat%C3%A9gories_de_cellules_qui_se_sous-divisent_en_types_de_cellules_sp%C3%A9cifiques_avec_des_r%C3%B4les_pr%C3%A9cis7.gif?wprov=srpw1_75
39. Figure 4: [cited 08.08.2020]
Different Stem- Cell possibilities in a placenta, adapted from:
https://upload.wikimedia.org/wikipedia/commons/thumb/6/66/Placenta_%28PSF%29.png/896px-Placenta_%28PSF%29.png
40. Figure 7: [cited 08.08.2020]
Schematic illustration of Vena sublingualis, available at:
https://www.ibyme.org.ar/archivos/laboratorios/adjuntos/poe-vias-de-extraccion.pdf